An Inhibitory Function of TRPA1 Channels in TGF-β1-driven Fibroblast to Myofibroblast Differentiation

Fabienne Geiger[1], Sarah Zeitlmayr[1], Claudia A. Staab-Weijnitz[2], Suhasini Rajan[1], Andreas Breit[1], Thomas Gudermann[1], Alexander Dietrich[1]

[1] Walther Straub Institute of Pharmacology and Toxicology, Member of the German Center for Lung Research (DZL), LMU-Munich, Munich Germany.

[2] Comprehensive Pneumology Center with the CPC-M BioArchive and Institute of Lung Health and Immunity, Helmholtz-Zentrum München, Member of the German Center of Lung Research (DZL), Munich, Germany

Conflict of interest: The authors have declared that no conflict of interest exists.

Address correspondence to: Alexander Dietrich, Walther-Straub-Institute of Pharmacology and Toxicology, Medical Faculty, LMU-Munich, Nussbaumstr. 26, 80336 Munich, Germany. Phone + 49 89 2180 73802; Fax + 49 89 2180 73817, Email:

Alexander.dietrich@lrz.uni-muenchen.de

ORCID IDs:

Fabienne Geiger: 0000-0002-7550-9739

Claudia Staab-Weijnitz: 0000-0002-1211-7834

Andreas Breit: 0000-0002-9343-2798

Alexander Dietrich: 0000-0002-1168-8707

Author Contributions: Conception and design: F.G. and A.D. Data acquisition and interpretation: F.G., S.Z., C.A.S.-W., S.R., A.B. and A.D. Drafting and revision of manuscript: F.G., S.Z., C.A.S.-W., S.R., A.B., T.G. and A.D.

Keywords: pulmonary fibrosis, ERK1/2, MAPK p38, plasminogen activator inhibitor-1 (PAI-1)

Abstract

Transient receptor potential ankyrin 1 (TRPA1) is a non-selective Ca^{2+} permeable cation channel, which was originally cloned from human lung fibroblasts (HLFs). TRPA1-mediated Ca^{2+} entry is evoked by exposure to several chemicals, including allyl isothiocyanate (AITC), and a protective effect of TRPA1 activation in the development of cardiac fibrosis has been proposed. Yet, the function of TRPA1 in transforming growth factor β1 (TGF-β1)-driven fibroblast to myofibroblast differentiation and the development of pulmonary fibrosis remains elusive. TRPA1 expression and function was analyzed in cultured primary HLFs, and mRNA levels were significantly reduced after adding TGF-β1. Expression of genes encoding fibrosis markers, e.g. alpha smooth muscle actin (*ACTA2*), plasminogen activator inhibitor 1 (*SERPINE1*), fibronectin (*FN1*) and type I collagen (*COL1A1*) was increased after siRNA-mediated down-regulation of TRPA1-mRNA in HLFs. Moreover, AITC-induced Ca^{2+} entry in HLFs was decreased after TGF-β1 treatment and by application of TRPA1 siRNAs, while AITC treatment alone did not reduce cell viability or enhanced apoptosis. Cell barrier function increased after addition of TRPA1 siRNAs or TGF-β1 treatment. Most interestingly, AITC-induced TRPA1 activation augmented ERK1/2 phosphorylation, which might inhibit TGF-β-receptor signaling. Our results suggest an inhibitory function of TRPA1 channels in TGF-β1-driven fibroblast to myofibroblast differentiation. Therefore, activation of TRPA1 channels might be protective during the development of pulmonary fibrosis in patients. (213 words)

(Word count: Abstract (213), Introduction (686), Materials and Methods (447 words, only Cells, RNA-Seq, Plasmin Assay, Electroporation), Results and Discussion (1957)

Introduction

Lung fibrosis is a chronic progressive disease with limited medical treatment options, leading to respiratory failure and death with a median overall survival time of 3-5 years after diagnosis (1). The most progressive form of the disease is idiopathic pulmonary fibrosis (IPF) (2), a chronic fibrotic interstitial lung disease of unknown cause, which occurs primarily in older adults (3). The incidence of IPF appears to be higher in North America and Europe (3 to 9 cases per 100,000 person-years) than in South America and East Asia (fewer than 4 cases per 100,000 person-years) (4).

The role of inflammation of lung tissues in IPF has been discussed extensively (5). However, multiple and potent anti-inflammatory therapies, in particular corticosteroids, have failed to show benefits in patients with IPF (5). The recently in the US approved drug pirfenidone down-regulates the production of growth factors like TGF-β1 and procollagens, whereas the already established nintedanib is a multi-tyrosine-kinase inhibitor. Both compounds slow down the decrease of forced vital capacity and also improve patients' quality of life, but do not increase survival rates (6, 7). Therefore, the need for more causative acting drugs directed against novel identified pharmacological targets is obvious.

Although the detailed molecular steps of fibrosis development are still elusive, it is now generally thought that, after chronic microinjuries, epithelial cells release mediators like TGF-β1, which induce fibroblast to myofibroblast differentiation (1, 2). Myofibroblasts express more α-smooth muscle actin (α-SMA) and secrete extracellular matrix (ECM) proteins (e.g. collagen (COL), fibronectin 1 (FN1) and plasminogen-activator-inhibitor 1 (PAI-1)) for the recovery of lung barrier function (1, 2). Indeed, IPF is characterized by scattered accumulation of myofibroblasts in fibroproliferative foci with ECM, which results in irreversible destruction of lung architecture and seriously inhibits alveolar gas

exchange in patients (1, 7). In addition to fibroblasts, alveolar epithelial cells (8, 9), fibrocytes (10), pericytes (11) and pleural mesothelial cells (12) may also, at least in part, transdifferentiate to myofibroblasts.

The superfamily of transient receptor potential (TRP) channels of vertebrates consists of 28 members in six families fulfilling multiple roles in the living organism (13). While TRPC6, the 6th member of the classical or canonical TRPC family, is activated by ligand binding (14), TRPV4, a channel of the vanilloid family, is thermosensitive in the range from 24 to 38 °C, and may serve as mechanosensor because it is activated by membrane and shear stretch (15). Both proteins form tetrameric unselective cation channels, which are expressed in human and mouse fibroblasts (16-18) and increase intracellular Ca^{2+} and Na^{+} levels initiating multiple signal transduction pathways and cellular responses (13). Most interestingly, TRPV4 has already been identified as an important player in pulmonary fibrosis in mice, and its expression was upregulated in lung fibroblasts derived from IPF patients (18). Moreover, we were able to show that mice lacking TRPC6 were partly protected from bleomycin-induced lung fibrosis (17). TRPC6 channel expression was increased in primary murine lung fibroblasts after application of TGF-β1, and ablation of TRPC6 resulted in reduced α-SMA production, less migration of myofibroblasts as well as in decreased secretion of ECM (17). Therefore, TRPV4 and TRPC6 are important determinants of TGF-β1-induced myofibroblast differentiation during fibrosis in mice.

Here, we set out to analyze TRP mRNA expression patterns in primary human lung fibroblasts (HLFs) with and without incubation with TGF-β1 in a more translational approach. While TRPC6 and TRPV4 mRNA expression was not changed, we identified a TGF-β1-mediated down-regulation of TRPA1, another member of the TRP superfamily. TRPA1, which is the only member of the TRPA family, harbors many

ankyrin repeat domains in its amino-terminus and opens its pore after exposure to several chemicals including AITC (19). Most interestingly, steroids and pirfenidone, a drug used as therapeutical option in patients with lung fibrosis, also activated TRPA1 channels, which resulted in inhibition of trinitrobenzene-sulfonic-acid–induced colitis (20). Moreover, calcitonin-gene-related peptide (CGRP) production after activation of TRPA1 channels in cardiac fibroblasts worked as an endogenous suppressor of cardiac fibrosis (21).

SiRNA-mediated down-regulation of TRPA1 mRNA resulted in up-regulation of mRNA and protein expression of pro-fibrotic marker proteins. AITC-induced increases in intracellular Ca^{2+} levels [$(Ca^{2+})_i$] were reduced and cell barrier function was increased after application of TRPA1 siRNAs. Moreover, TGF-β1-signaling was decreased by AITC-induced TRPA1 activation, probably by ERK phosphorylation and SMAD2 linker phosphorylation. Therefore, in contrast to TRPC6 and TRPV4, TRPA1 channels are able to inhibit fibroblast to myofibroblast differentiation and may serve as pharmacological targets in the development of new therapeutic options for pulmonary fibrosis.

Material and Methods

Cells

HLFs of healthy donors were obtained from Lonza (Basel, Switzerland, #CC-2512), PromoCell (Heidelberg, Germany, #C-12360) or from the CPC-M BioArchive for lung diseases at the Comprehensive Pneumology Center (CPC Munich, Germany). HLFs were used until passage 8. Ethical statements were provided by the suppliers.

Transcriptomic Analysis by RNA-Seq

HLFs were incubated with TGF-β1 or solvent as described in the Data Supplement and RNA-seq was performed by IMGM Laboratories (Martinsried, Germany) on the Illumina NovaSeq® 6000 next generation sequencing system as described (22). Data for normalized counts and differential gene expression were obtained with the bioconductor package DESeq2 (23) and gene enrichment analysis with ClusterProfiler (24) in R version 4.1.2. The dataset has been deposited in the ArrayExpress database at EMBL-EBI (www.ebi.ac.uk/arrayexpress) under accession number E-MTAB-11629.

Plasmin Assay

To indirectly quantify the secretion of PAI-1 from HLFs, 10 µl of the supernatant of HLFs, 10 µL of 10 mM of D-Val-Leu-Lys 7-amido-4-methylcoumarin (D-VLK-AMC) (in 10 % DMSO/H2O) (Sigma-Aldrich, #V3138) as plasmin substrate (25) and 80 µL TRIS/HCl (20 mM, pH7.4) were incubated for 4 h at 37 °C, 5 % CO2 in a black 96-wellplate with clear bottom. Fluorescence intensity of AMC was measured at λ_{ex} 380 nm; λ_{em} 460 nm using a TECAN plate reader (Tecan, Infinite M200 Pro). Higher fluorescence values indicate increased levels of plasmin processed by t-PA, as D-VLK-AMC is hydrolyzed by plasmin to AMC (26).

Electroporation and Luciferase Reporter Assay

HLFs were electroporated with the Neon® Transfection system to achieve plasmid transfection as described (27). 250,000 HLFs were resuspended in 100 µL buffer R (Neon™ Transfection System 100 µL Kit, Invitrogen, MPK10096) and 4 µL of the Luciferase Reporter Plasmid (1 µg/µL pGL3-CAGA(9)-luc) containing the SMAD-sensitive part of the human PAI-1 promotor controlling the luciferase gene (28) was added. The electroporation was performed with 1400 Volt, 2 pulses à 20 ms. . HLFs were seeded in four wells of a 24-well plate in antibiotic free medium containing 2 % (Lonza, PromoCell) or 10 % (DZL) serum. After 24 h, the cells were treated with TGF-β1 (2 ng/mL) or solvent, medium contained 1 % Penicillin/ Streptomycin and 0.1 % serum. On the second day, the cells were pretreated with A-967079 (500 nM) or solvent for 30 min and stimulated with AITC (10 µM), JT010 (75 nM) or DMSO for 120 min. The fibroblasts were lysed in 50 µl lysis buffer per well (25 mM Tris/HCl pH7.4, 4 mM EGTA, 8 mM MgCl2, 1 mM DTT, 1 % Triton X-100) for 10 min. at RT. Luminescence was measured upon injection of 20 µl luciferase reporter assay substrate (Promega, #E1501) to each well using an OMEGA plate reader.

All other Methods are described in the Data Supplement, which is available online.

Results

Transcriptional and Functional Down-Regulation of TRPA1 Channels in Human Lung Fibroblasts (HLFs) after Application of TGF-β1

To investigate the role of TRP channels in TGF-β1-driven fibroblast to myofibroblast differentiation, we cultured primary HLFs from three human donors, applied TGF-β1 (2 ng/ml for 48 h) or solvent and extracted RNA for a thorough transcriptomic analysis. While mRNAs coding typical marker proteins for lung fibrosis and signaling pathways for extracellular matrix and structure organization were significantly up-regulated (*see* Figure E1A, B), none of the channels of the TRPC, TRPV and TRPM families showed significant changes in their mRNA expression levels after application of TGF-β1 (*see* Figure E1C-E). For TRPA1 mRNA, however, there was a clear trend for a TGF-β1-induced down-regulation (*see* Figure E1F), which turned out to be significant in a comparison of log2 fold changes (Table 1). Moreover, this significant reduction of TRPA1 mRNA after application of TGF-β1 was reproducible by repetitive quantitative RT-PCR experiments (Figure 1A). To successfully manipulate TRPA1 expression in lung fibroblasts, we tested an siRNA pool directed against TRPA1 mRNA and identified an 84,4 % down-regulation of TRPA1 mRNA, while a scrambled control siRNA showed no significant changes (Figure 1A). We tested four TRPA1 antisera, including two monoclonal antibodies reported to be selective for TRPA1 channels (29). However, in our hands these batches of antibodies showed no selectivity for the TRPA1 protein in HEK293 cells stably expressing the channel (*see* Figure E2). Therefore, TRPA1 function was analyzed by Ca^{2+} imaging of fibroblasts. Application of the specific TRPA1 activator, AITC, resulted in a transient increase of the intracellular Ca^{2+} concentration ($(Ca^{2+})_i$), which was reduced in cells transfected with TRPA1 siRNAs (Figure 1B, C). Most interestingly, fibroblasts treated with TGF-β1 showed significantly reduced AITC-

induced increases in $(Ca^{2+})_i$ in comparison to control cells incubated with solvent only (Figure 1D, E). We obtained similar results with another specific activator of TRPA1 channels JT010 (30)(*see* Figure E3A-B). Therefore, TRPA1 expression and function is reduced after application of TGF-β1 to primary human fibroblasts. This AITC-induced increase in $(Ca^{2+})_i$ was blocked by a specific TRPA1 inhibitor, A-967079 (A96), in the absence and presence of TGF-β1 (*see* Figure E3C, D).

Down-Regulation of TRPA1 mRNA Increases Expression of Fibrosis Markers in HLFs

TGF-β1-induced fibroblast to myofibroblast differentiation is a key event in the development of lung fibrosis and results in up-regulation of gene expression of *ACTA2*, *COL1A1*, *FN1* and *SERPINE1*, encoding the fibrotic marker proteins α-smooth muscle actin (α-SMA), the α(1) chain of type I collagen (COL1A1), fibronectin 1 (FN-1) and plasminogen activator inhibitor 1 (PAI-1), respectively. As expected, application of TGF-β1 resulted in up-regulation of mRNA expression from these genes (Figure E1A). Most interestingly, transfection of cells by the specific TRPA1 siRNA but not a control siRNA was also able to increase mRNA expression of fibrotic marker proteins in the absence of TGF-β1 (Figure 2A-D). To evaluate these small but significant increases in mRNA levels on a protein level, we performed quantitative Western Blotting of protein lysates from fibroblasts transfected with TRPA1-specific or control siRNA. Expression of both proteins α-SMA and COL1A1increased after down-regulation of TRPA1 channels (Figure 2E-H). TRPA1-specific siRNA was however not effective, if cells were preincubated with TGF-β1 (see Figure E4A, B). Thus, in turn, TRPA1 expression and function seems to suppress expression of pro-fibrotic genes.

Down-Regulation of TRPA1 mRNA Increase and Application of TRPA1 Activators Decrease Function of Pro-Fibrotic Proteins in HLFs

To further evaluate effects of TRPA1 channels on protein expression and function, we performed several assays. Detection of α-SMA by binding of an α-SMA-specific antibody followed by a fluorophore-coupled secondary antibody revealed increased protein levels after TGF-β1-induction in HLFs, which were also identified after application of the TRPA1 siRNA (Figure 3A, B). Phalloidin-staining to detect F-actin was also enhanced after incubation of cells with TGF-β1 or TRPA1 siRNA (Figure 3C, D). TGF-β1-induced up-regulation of α-SMA and collagen 1A1 (COL1A1) was detected by Western blotting in HLFs and was significantly down-regulated by the TRPA1 activator AITC (Figure 3E-H). We obtained similar results in the presence of the other specific TRPA1 activator JT010 and co-treatment with TGF-β1 (*see* Figure E4C-F). PAI-1 is able to inhibit tissue plasminogen activator (t-PA) or urokinase (uPA)-induced production of plasmin, which results in degradation of fibrin clots (Figure 4A). This process is quantified by cleaving of D-Val-Leu-Lys 7-amido-4-methylcoumarin (D-VLK-AMC) by plasmin and increased emission of fluorescence from free AMC (Figure 4B) (26). As expected, plasmin-induced fluorescence of the HLF medium was decreased after incubation of cells with TGF-β1. Transfection of cells with TRPA1 siRNA, was also able to decrease fluorescence, although to a lesser extent (Figure 4C). Application of the TRPA1 activators AITC (Figure 4D) or JT010 (*see* Figure E4G) also resulted in a lesser or no decrease in plasmin activity, respectively. In conclusion, down-regulation of TRPA1 results in higher expression and activity of pro-fibrotic marker proteins, while treatment of HLFs with TRPA1 activators resulted in decreased plasmin activity most probably by a reduced expression of PAI-1.

~~**Down-Regulation of TRPA1 mRNA Results in Increased Cell Resistance of HLFs**~~

~~Lung fibrosis due to myofibroblast accumulation results in increased lung resistance. Along this line, we quantified cell barrier function in an ECIS system. Cell resistance increased after TGF-β1 treatment, most probably due to augmented α-SMA levels and production of ECM proteins like collagen and FN1 (Figure 5A, B). Most interestingly, application of TRPA1 siRNA to the extracellular medium also resulted in a significant increase in cell resistance (Figure 5C, D). In conclusion, down-regulation of TRPA1 mRNA changes cell barrier behavior of HLFs.~~

TRPA1-Induced MAPK Phosphorylation Inhibits TGF-β1-mediated Transcription of Fibrotic Marker Proteins

To understand TRPA1 channel and TGF-β1 function on cellular transcription levels, we established a luciferase assay. A construct, containing luciferase cDNA under the control of *SERPINE1* (encoding PAI-1) core promoter region (pGL3-CAGA(9)-luc) (28), was transfected in HLFs. Cells were treated with TGF-β1, AITC, the TRPA1 inhibitor A-967079, or a combination of all three compounds (Figure 5A), and luciferase activity was quantified. As expected, application of TGF-β1 resulted in increased PAI-1 promoter-induced luciferase activity as compared to treatment with solvent only. Incubation of cells with AITC for 2 h, however, reduced TGF-β1-induced luciferase activity, which returned to initial levels if A-967079 was applied (Figure 5B). This inhibition of gene transcription was not due to cell apoptosis or reduced cell viability, as caspase and WST assays showed no increased apoptosis or reduced cell viability by AITC treatment, respectively (*see* Figure E8). TGF-β1 signaling via SMAD isoforms and inhibition of SMAD-dependent transcription by the MAPK signaling pathway has been reported in a fetal lung epithelial cell line (31, 32). Moreover, increased

expression of pro-fibrotic markers by ERK inhibition was recently shown in dermal fibroblasts (33). Therefore, we quantified ERK1/2 and MAPK p38 phosphorylation in response to application of TGF-β1, AITC and TRPA1 siRNA by Western-analysis using a phospho-specific ERK1/2 antibody. AITC was able to increase ERK1/2 phosphorylation as reported before (34) as well as MAPK p38, which was reduced to basal levels after pre-incubation with TRPA1 siRNA (Figure 5C, D and Figure E5A-B). Pre-incubation with TGF-β1 resulted in ERK1/2 and MAPK p38 phosphorylation after application of TRPA1 siRNA or AITC, which however were not significantly different (see Figure E5C-F). Removal of extracellular Ca^{2+} reduced AITC-induced ERK1/2 and MAPK p38 phosphorylation to basal levels (see Figure E6A-D). TGF-β1 regulated transcription is mediated by carboxy-terminal phosphorylation of SMAD2/3 proteins, which are subsequently translocated to the nucleus. Additional phosphorylation of serine residues (245, 250, 255) in the linker region of SMAD2 proteins, however, results in inhibition of nuclear translocation ((31, 32) and reviewed in (35)). To dissect the signaling pathway mediating TRPA1-induced inhibition of TGF-β1 signaling in human fibroblasts, we analyzed linker phosphorylation of SMAD2 proteins in HLFs after stimulation by AITC by Ser245/250/255 specific phospho-SMAD2 antibodies. Most interestingly, application of AITC (3 μM) for 10 min. resulted in an increase in SMAD2 linker phosphorylation, which was found to be reduced after a longer incubation time of 30 min. and by simultaneous application of the TRPA1 inhibitor A567079 (Figure 5E, F). Preincubation with TGF-β1 also resulted in changes in SMAD2 linker phosphorylation after application of AITC, which however were not significantly different (see Figure E7A). Removal of extracellular Ca^{2+} reduced AITC-induced SMAD2 linker phosphorylation to basal levels (see Figure E7B,C). Previous studies revealed that sustained stimulation of MRC5 cells or HLFs with TGF-β1 reduced total protein levels of SMAD3 (36, 37). We also observed a profound reduction

of cytosolic SMAD3 levels after TGF-β1 stimulation of HLFs (*see* Fig. E7D, E). Interestingly, application of AITC significantly increased basal SMAD-3 levels (*see* Fig. E6B, C) confirming an important function of TRPA1 activation also on SMAD3.

In conclusion, our data favor a mechanistic model in which TRPA1 mediated ERK phosphorylation inhibits TGF-β1-induced transcription and fibroblast to myofibroblast differentiation by linker phosphorylation of SMAD2 proteins (Figure 6).

Discussion

Pulmonary fibrosis is a devastating disease with only a few treatment options. Although detailed molecular aspects of the development of lung fibrosis are still elusive, it is commonly believed that fibroblast to myofibroblast differentiation is a decisive step. The identification of new target proteins mediating this process is therefore an important step toward establishing new biomarkers and future therapeutic options. TRP-channels are expressed and essential for Ca^{2+} homeostasis in many cells including fibroblasts (17, 38). We were able to demonstrate an essential role of the classical TRP channel 6 (TRPC6) in murine fibroblast to myofibroblast differentiation (17). On a molecular level, TRPC6 mRNA and protein levels were up-regulated in myofibroblasts compared to fibroblasts and TRPC6 deficient mice were partially protected from bleomycin-induced pulmonary fibrosis (17). Moreover, expression of TRPV4, a member of the vanilloid family of TRP channels, was up-regulated in lung fibroblasts derived from IPF patients (18). However, after a thorough transcriptomic comparison of primary human fibroblasts with TGF-β1-differentiated myofibroblasts, we were not able to identify significantly different TRPC6 or TRPV4 mRNA expression levels. Most interestingly and contrary to mRNAs of all other TRP proteins, TRPA1 mRNA was found to be significantly down-regulated (Table 1). TRPA1 channels were originally identified in human fibroblasts (19). In addition, they are important sensor

molecules for toxicants (39, 40). While the exact triggers for the development of lung fibrosis are still not known, it is believed that microinjuries of epithelial cells by chronic exposure to lung toxicants are an important predisposition for the disease (1, 7).

For the first time, we present evidence for an inhibitory role of TRPA1 channels in primary HLF to myofibroblast differentiation by TGF-β1. Preincubation of cells with TGF-β1 decreased AITC-induced increases in $(Ca^{2+})_i$ (Figure 1D, E). A specific knockdown of TRPA1 expression increased mRNA (Figure 2A-D) and protein expression (Figure 2E-H) of important pro-fibrotic marker proteins, reduced AITC-induced increases in intracellular Ca^{2+} levels (Figure 1B-C) ~~and increased cell resistance (Figure 5C-D)~~. Most interestingly, we were able to monitor basal TRPA1 activity in HLFs, probably protecting these cells from myofibroblast differentiation. Of note, pre-application of TGF-β1 and TRPA1 siRNA had no additive effect on the expression of fibrotic genes (e.g. α-SMA and COL1A1 (Figure E4A, B), as TRPA1 mRNA might be already down-regulated in cells treated with TGF-β1. However, co-application of TGF-β1 and AITC or JT010 activated TRPA1 channels in the cell membrane with a high efficacy and reduced TGF-β1-mediated gene transcription and PAI-1 activity (Figure 5B, 4D and E4G) as well as expression of fibrotic proteins (e.g. COL1A1 and α-SMA in Figure 3E-H and E4C-F). On a molecular level, TRPA1 channel activation by AITC induced ERK1/2 phosphorylation (Figure 5C, D) and SMAD2 linker phosphorylation (Figure 5E, F), which reduces nuclear translocation and activation of transcription ((32) reviewed in (35)). Down-regulation by specific TRPA1 siRNAs or a TRPA1 inhibitor reversed these effects (Figure 5C-F). Moreover, depletion of extracellular Ca^{2+} reduced AITC-induced phosphorylation of ERK1/2, MAPKp38 and the SMAD2 linker region, supporting the notion that phosphorylation of these proteins depend on AITC-mediated increase of $[Ca^{2+}]_i$. These findings highlight an inhibitory

role of TRPA1 in the development of human myofibroblasts triggered by TGF-β1. In a recent publication, a similar effect was shown in MRC-5 and HF19 cell lines, which are both isolated from lungs of human fetuses and resemble some of the characteristics of human fibroblasts (41). TGF-β1 significantly down-regulated TRPA1 expression and AITC enhanced α-SMA gene and protein expression in these cell lines (41). HC-030031 as a TRPA1 antagonist however, failed to suppress the AITC-induced down-regulation of α-SMA and seemed to work synergistically with AITC (41). Only combined inhibition of ERK1/2 mitogen activated protein kinase (MAPK) and nuclear factor of erythroid 2-related factor (NERF) reversed the AITC-induced α-SMA suppression (41).

While this work was in progress, another research group investigated TRPA1 channels in human lung myofibroblasts (HLMFs) and TGF-β1-mediated pro-fibrotic responses (42). The researchers reported that the expression and function of TRPA1 channels in both healthy and IPF patients were reduced by application of TGF-β1 (42). TRPA1 over-expression or activation induced HLMF apoptosis, and TRPA1 activation by H_2O_2 induced necrosis. TRPA1 inhibition resulting from TGF-β1 down-regulation or pharmacological inhibition protected HLMFs from both apoptosis and necrosis (42). They concluded that TGF-β1 induces resistance of HLMFs to TRPA1 agonist- and H_2O_2-mediated cell death via down-regulation of TRPA1 (42). These data in human myofibroblasts confirm our results, underscoring an inhibitory role of TRPA1 in pro-fibrotic events governing fibroblast to myofibroblast differentiation at an early stage of lung fibrosis. However, there are also clear differences in the role of TRPA1 channels in HLFs versus HMLFs. We did not observe any reduction in cell viability or increases in apoptosis in human lung fibroblasts after activation of TRPA1 by the specific activator AITC (*see* Figure E8), while overexpression of TRPA1 in HLMFs increased

apoptosis (42). However, we did not use H_2O_2, as this compound also activates TRPM2 channels and can induce cell death *per se* (43).

There is also evidence that TRP channels cluster with other signaling molecules in compartments formed by proteins like caveolins (44). In these caveolae as microdomains of calcium signaling (45), Ca^{2+} influx through TRPA1 channels might indeed inhibit fibroblast to myofibroblast differentiation, while in others Ca^{2+} influx through TRPV4 channels might promote lung fibrosis (18).

As it is generally accepted that fibroblasts mainly contribute to the progression of pulmonary fibrosis by differentiating to myofibroblasts and secreting excessive amounts of ECM (46), our data in HLFs and the results of others in HLMFs point to an important inhibitory function of TRPA1 channels in fibroblast to myofibroblast differentiation and HLMFs survival. Therefore, activation of TRPA1 channels may blaze the trail for new therapeutic options in lung fibrosis. Future studies will show, if TRPA1 activators are successful in fibrosis models, despite their effects on other cells (e.g. neurons), where TRPA1 channels are also expressed.

Table 1:

TRP Channel	Log2 fold change	*P*-value	Adjusted *P*-value
TRPA1	-1.649	**0.003**	**0.047**
TRPC1	-0.437	0.262	0.675
TRPC2	n. a.	n. a.	n. a.
TRPC3	0.173	0.842	0.969
TRPC4	-0.788	0.523	0.860
TRPC5	0.528	0.807	n. a.
TRPC6	-0.205	0.728	0.939
TRPC7	n. a.	n. a.	n. a.
TRPM1	-1.531	0.705	n. a.
TRPM2	1.239	0.761	n. a.
TRPM3	-0.868	0.499	n. a.
TRPM4	0.037	0.932	0.992
TRPM5	n. a.	n. a.	n. a.
TRPM6	-0.793	0.700	n. a.
TRPM7	0.001	0.997	1.000
TRPM8	-0.525	0.755	n. a.
TRPV1	-0.048	0.931	0.991
TRPV2	-0.618	0.433	0.809
TRPV3	1.693	0.214	n. a.
TRPV4	0.259	0.821	0.964
TRPV5	n. a.	n. a.	n. a.
TRPV6	1.239	0.761	n. a.

Table 1: Log2 fold changes and *P*-values for TRP channel mRNA expression obtained by transcriptomic analysis of human lung fibroblasts treated with TGF-β1 or solvent. *P*-values < 0.05 are indicated in **bold**. n.a, not available

Figure legends

Figure 1: Quantitative reverse transcription (qRT)-PCR and Ca^{2+} imaging in primary human lung fibroblasts (HLFs) cultured with TGF-β1 or transfected with TRPA1-specfic siRNAs. (*A*) TRPA1 mRNA expression quantified by qRT-PCR experiments in HLFs cultured with TGF-β1 (+ TGF-β1) or transfected with TRPA1 specific siRNAs (siTRPA1). Solvent (Solv.) or scrambled siRNAs (siCtrl.) served as controls. (*B*) HLFs were transfected with TRPA1 specific siRNAs (siTRPA1, blue line) or scrambled siRNAs (siCtrl., grey line) as a control and intracellular Ca^{2+} levels were quantified as normalized ratios 340/380 nm after adding the TRPA1 activator AITC (10 µM) as

described in Materials and Methods. Light grey areas represent SEM. (*C*) Areas under the curves were calculated and plotted as bars (siTRPA1, blue bar; siCtrl., black bar). (*D*) HLFs were cultured with TGF-β1 (+ TGF-β1, red line) or solvent (Solv., black line) as a control and intracellular Ca^{2+} levels were quantified as normalized ratios 340/380 nm after adding the TRPA1 activator AITC (10 µM) as described in the Data Supplement. Light grey areas represent SEM. (*E*) Areas under the curves were calculated and plotted as bars (+ TGF-β1, red bar; Solv., black bar). Data were analyzed by a Kruskal-Wallis (*A*) or a Mann-Whitney test (*C+E*) and are presented as mean ± SEM. qRT-PCR and Calcium Imaging experiments were performed with n ≥ 5 independent cell isolations each. For all graphs, *P < 0.05, ***P < 0,001, ****P <0.0001 versus the value in cells treated with solvent or scrambled siRNA alone.

Figure 2: Quantitative reverse transcription (qRT)-PCR and Western-Blotting experiments for expression of fibrotic marker genes in human lung fibroblasts (HLFs) cultured with TGF-β1 or transfected with TRPA1-spefic siRNAs. (*A*) Quantification of mRNA levels of *α-SMA* (*ACTA2*) in HLFs cultured with TGF-β1 (+ TGF-β1) or solvent (Solv.) as well as transfected with TRPA1 specific siRNAs (siTRPA1) or scrambled siRNAs (siCtrl.) as control. (*B*) Quantification of mRNA levels of collagen 1A1 (*COL1A1*) in HLFs cultured with TGF-β1 (+ TGF-β1) or solvent (Solv.) as well as transfected with TRPA1 specific siRNAs (siTRPA1) or scrambled siRNAs (siCtrl.) as control. (*C*) Quantification of mRNA levels of fibronectin (*FN1*) in HLFs cultured with TGF-β1 (+ TGF-β1) or solvent (Solv.) as well as transfected with TRPA1 specific siRNAs (siTRPA1) or scrambled siRNAs (siCtrl.) as control. (*D*) Quantification of mRNA levels of plasminogen activator inhibitor (*SERPINE1*) in HLFs cultured with TGF-β1 (+ TGF-β1) or solvent (Solv.) as well as transfected with TRPA1 specific

siRNAs (siTRPA1) or scrambled siRNAs (siCtrl.) as control. (*E, F*) Quantification of α-smooth muscle actin (α-SMA) protein levels in HLFs transfected with TRPA1 specific siRNAs (siRNA TRPA1) or scrambled siRNAs (siRNA Ctrl.) as control by quantitative Western-Blotting. (*G, H*) Quantification of collagen1A1 (COL1A1) protein levels in HLFs transfected with TRPA1 specific siRNAs (siRNA TRPA1) or scrambled siRNAs (siRNA Ctrl.) as control by quantitative Western-Blotting. Data were analyzed by a Kruskal-Wallis (*A-D*) or a Mann-Whitney test (*F, H*) and are presented as mean ± SEM. Cells are from at least three independent donors (n ≥ 4). For all graphs, *P < 0.05, **P < 0.01,***P < 0.001, ****P <0.0001 versus the value in cells treated with solvent or scrambled siRNA alone.

Figure 3: Quantification of expression of fibrotic marker proteins in human lung fibroblasts (HLFs) cultured with or without TGF-β1 and transfected with TRPA1-specific siRNAs or stimulated with the TRPA1 activator AITC. (*A*) Representative confocal laser microscopy images of HLF cultured with solvent (Solv.), TGF-β1 (+ TGF-β1), scrambled siRNA (siCtrl) or TRPA1-specific siRNA (siTRPA1) and stained with fluorophore-tagged anti α-smooth muscle actin antibodies (α-SMA ab). Scale bars, 50 µm. (*B*) Summary of mean gray values obtained from images shown in A. (*C*) Representative confocal laser microscopy images of HLFs cultured with solvent (Solv.), TGF-β1 (+ TGF-β1), scrambled siRNA (siCtrl) or TRPA1-specific siRNA (siTRPA1) and stained with fluorophore-tagged phalloidin for detection of F-actin. Scale bars, 50 µm. (*D*) Summary of mean gray values obtained from images shown in C. (*E*) α-smooth muscle actin (α-SMA) protein expression was quantified by Western blotting using a specific antiserum in HLFs cultured with or without TGF-β1 and/or treated with the TRPA1 activator AITC. Alpha-tubulin served as loading control. (*F*) Summary of α-SMA protein expression normalized to β-actin in HLFs cultured with or

without TGF-β1 and/or treated with the TRPA1 activator AITC in the indicated concentrations. (*G*) Collagen 1A1 (COL1A1) protein expression was quantified by Western blotting using a specific antiserum in HLFs cultured with or without TGF-β1 and/or treated with the TRPA1 activator AITC in the indicated concentrations. Alpha-tubulin served as loading control. (*H*) Summary of collagen 1A1 (COL1A1) protein expression normalized to β-actin in HLFs cultured with or without TGF-β1 and/or treated with the TRPA1 activator AITC in the indicated concentrations. Data were analyzed by analyzed by a Kruskal-Wallis test (*B, D*) or two-way ANOVA (*F, H*) and are presented as mean ± SEM. Cells in A-F are from at least three independent donors and the number of experiments is n ≥ 4. For all graphs, *P < 0.05, **P < 0.01,***P < 0.001, ****P <0.0001 versus the value in cells treated with solvent or scrambled siRNA alone.

Figure 4: Indirect quantification of expression of plasminogen-activator-inhibitor 1 (PAI-1) activity in human lung fibroblasts (HLFs) cultured with TGF-β1 or transfected with TRPA1-specific siRNAs. (*A*) Schematic picture of PAI-1 inhibits cleavage of plasminogen in plasmin by tissue plasminogen activator (t-PA). Plasmin is able to degrade fibrin clots during fibrinolysis. (*B*) Hydrolysis of DVLK-AMC by t-PA results in free AMC, which is quantified by fluorometric detection (excitation 380 nm, emission 460 nm). (*C*) Plasmin activity quantified by AMC fluorescence in the medium of HLFs cultured with solvent (Solv.) or TGF-β1 (+ TGF-β1) and transfected with scrambled siRNA (siCtrl) or TRPA1-specific siRNA (siTRPA1). (*D*) Plasmin activity quantified by AMC fluorescence in the medium of HLFs cultured with (+) or without (-) TGF-β1 and with (+) or without application of the TRPA1 activator AITC. Data were analyzed by y a Kruskal-Wallis test (*C*) or two-way ANOVA (*D*) and are presented as mean ± SEM. Cells are from at least three independent donors and number of experiments n ≥ 4. For

all graphs, *P < 0.05, **P < 0.01,***P < 0.001, ****P <0.0001. In graph C, for the value of cells treated with control versus the cells treated TGF-β1 or scrambled siRNA alone. Graph D: Control versus AITC-treated cells.

~~**Figure 5:** Electric cell-substrate impedance sensing in human lung fibroblasts (HLFs) cultured with TGF-β1 or transfected with TRPA1-spefic siRNAs. (*A*) Normalized cell resistance in % of initial values were quantified as described in the Data Supplement in HLFs cultured with TGF-β1 (+ TGF-β1) or solvent (Solv.). Light grey areas represent SEM. (*B*) Areas under the curves were calculated and plotted as bars (+ TGF-β1, red bar; Solv., grey bar). (*C*) Normalized cell resistance in % of initial values were quantified as described in the Data Supplement in HLFs transfected with TRPA1 specific siRNAs (siTRPA1, blue line) or scrambled siRNAs (siCtrl., grey line). Light grey areas represent SEM. (*D*) Areas under the curves were calculated and plotted as bars (siTRPA1, blue bar; siCtrl., grey bar). Data were analyzed by by an unpaired t test and are presented as mean ± SEM. Cells in A-D are from at least three independent donors (n = 3). For all graphs, *P < 0.05, ****P <0.0001 versus the value in cells treated with solvent or scrambled siRNA alone.~~

Figure 5: Identification of proteins involved in TRPA1-mediated inhibition of TGF-β1-induced transcription. (*A*) Schematic presentation of luciferase reporter assay. HLFs were transfected with a plasmid containing the luciferase gene under the control of the SMAD-sensitive part of the human PAI-1 promoter. TGF-β1 agonist for activation of SMAD transcription as well as AITC as TRPA1 activator or A-967079 as channel inhibitors were added and luciferase activity was quantified. (*B*) SMAD transcriptional activity in HLFs quantified after culturing in solvent (black bars) or TGF-β1 (red bars) as well as treatment with AITC or A-967079. (*C*) Lysates from fibroblasts transfected

with TRPA1 specific (siRNA TRPA1) or scrambled siRNA (siRNA Ctrl.) and treated with (+) or without (-) AITC were incubated in a Western Blot of with specific antibodies directed against phosphorylated ERK1/2 (pERK1/2) and ERK1/2. Alpha-tubulin served as loading control. (*D*) Summary of the pERK1/2/ERK1/2 quantification normalized to alpha-tubulin by Western Blotting in HLFs transfected withTRPA1 specific siRNAs (siTRPA1, blue bars) or scrambled siRNAs (siCtrl., grey bars) incubated with (+) or without (-) AITC. (*E*) Lysates from fibroblasts pretreated with (+) or without (-) A-967079 and stimulated with (+) or without (-) AITC for the indicted times (min.) were incubated in a Western Blot of with specific antibodies directed against linker phosphorylated SMAD2 (pSMAD2) and SMAD2. Beta-actin served as loading control. (*F*) Summary of the pSMAD2/SMAD2 quantification normalized to β-actin by Western Blotting in HLFs pretreated with (+) or without (-) A-967079 and incubated with (+) or without (-) AITC. Data were analyzed by two-way ANOVA (*B, D*) or a Kruskal-Wallis test (*F*) and are presented as mean ± SEM. Cells in A-F are from at least three independent donors (n ≥ 3). For all graphs, *P < 0.05, ****P <0.0001 versus the value in cells treated with solvent alone.

Figure 6: Proposed signaling pathway for TRPA1-mediated inhibition of TGF-β1-induced SMAD-mediated transcription. Ca^{2+} influx through AITC- or JT010 activated TRPA1 channels increases ERK1/2 phosphorylation, which induces linker phosphorylation of SMAD2. In contrast to the carboxyterminal phosphorylation of SMAD2, which enhances nuclear SMAD-induced transcription by activated TGF-β-receptors, linker phosphorylation of SMAD2 reduces TGF-β1-induced transcription of profibrotic genes. A TRPA1 inhibitor (A-967079) is able to reverse the inhibitory effect of TRPA1-induced Ca^{2+} influx. Moreover, TRPA1 gene expression is inhibited by TGF-β1-activation of HLFs by a still unknown mechanism.

Acknowledgement: This study was funded by the Deutsche Forschungsgemeinschaft (TRR152 (P15, P16) and GRK 2338 (P04, P07, P10)) and the German Lung Center (DZL). The authors thank Bettina Braun and Astrid Bauer for excellent technical assistance and Anna Litovskikh for her great help in the analysis of transcriptomic data with R. We gratefully acknowledge the provision of human primary fibroblasts from the CPC-M bioArchive and its partners at the Asklepios Biobank Gauting, the Klinikum der Universität München, and the Ludwig-Maximilians-Universität München. Figures 6A and 7 have been created by BioRender.com.

References

1. King TE, Jr., Pardo A, Selman M. Idiopathic pulmonary fibrosis. *Lancet* 2011; 378: 1949-1961.
2. Lederer DJ, Martinez FJ. Idiopathic Pulmonary Fibrosis. *N Engl J Med* 2018; 378: 1811-1823.
3. Raghu G, Collard HR, Egan JJ, Martinez FJ, Behr J, Brown KK, Colby TV, Cordier JF, Flaherty KR, Lasky JA, Lynch DA, Ryu JH, Swigris JJ, Wells AU, Ancochea J, Bouros D, Carvalho C, Costabel U, Ebina M, Hansell DM, Johkoh T, Kim DS, King TE, Jr., Kondoh Y, Myers J, Muller NL, Nicholson AG, Richeldi L, Selman M, Dudden RF, Griss BS, Protzko SL, Schunemann HJ, Fibrosis AEJACoIP. An official ATS/ERS/JRS/ALAT statement: idiopathic pulmonary fibrosis: evidence-based guidelines for diagnosis and management. *American journal of respiratory and critical care medicine* 2011; 183: 788-824.
4. Hutchinson J, Fogarty A, Hubbard R, McKeever T. Global incidence and mortality of idiopathic pulmonary fibrosis: a systematic review. *Eur Respir J* 2015; 46: 795-806.
5. Selman M, King TE, Pardo A. Idiopathic pulmonary fibrosis: prevailing and evolving hypotheses about its pathogenesis and implications for therapy. *Annals of internal medicine* 2001; 134: 136-151.
6. Selvaggio AS, Noble PW. Pirfenidone Initiates a New Era in the Treatment of Idiopathic Pulmonary Fibrosis. *Annual review of medicine* 2015.
7. Martinez FJ, Collard HR, Pardo A, Raghu G, Richeldi L, Selman M, Swigris JJ, Taniguchi H, Wells AU. Idiopathic pulmonary fibrosis. *Nat Rev Dis Primers* 2017; 3: 17074.
8. Tanjore H, Cheng DS, Degryse AL, Zoz DF, Abdolrasulnia R, Lawson WE, Blackwell TS. Alveolar epithelial cells undergo epithelial-to-mesenchymal transition in response to endoplasmic reticulum stress. *J Biol Chem* 2011; 286: 30972-30980.
9. Bartis D, Mise N, Mahida RY, Eickelberg O, Thickett DR. Epithelial-mesenchymal transition in lung development and disease: does it exist and is it important? *Thorax* 2014; 69: 760-765.
10. Hashimoto N, Jin H, Liu T, Chensue SW, Phan SH. Bone marrow-derived progenitor cells in pulmonary fibrosis. *J Clin Invest* 2004; 113: 243-252.
11. Hung C, Linn G, Chow YH, Kobayashi A, Mittelsteadt K, Altemeier WA, Gharib SA, Schnapp LM, Duffield JS. Role of lung pericytes and resident fibroblasts in the pathogenesis of pulmonary fibrosis. *American journal of respiratory and critical care medicine* 2013; 188: 820-830.
12. Mubarak KK, Montes-Worboys A, Regev D, Nasreen N, Mohammed KA, Faruqi I, Hensel E, Baz MA, Akindipe OA, Fernandez-Bussy S, Nathan SD, Antony VB. Parenchymal trafficking of pleural mesothelial cells in idiopathic pulmonary fibrosis. *Eur Respir J* 2012; 39: 133-140.
13. Nilius B, Szallasi A. Transient receptor potential channels as drug targets: from the science of basic research to the art of medicine. *Pharmacological reviews* 2014; 66: 676-814.
14. Chen X, Sooch G, Demaree IS, White FA, Obukhov AG. Transient Receptor Potential Canonical (TRPC) Channels: Then and Now. *Cells* 2020; 9.
15. Goldenberg NM, Ravindran K, Kuebler WM. TRPV4: physiological role and therapeutic potential in respiratory diseases. *Naunyn Schmiedebergs Arch Pharmacol* 2015; 388: 421-436.
16. Davis J, Burr AR, Davis GF, Birnbaumer L, Molkentin JD. A TRPC6-dependent pathway for myofibroblast transdifferentiation and wound healing in vivo. *Developmental cell* 2012; 23: 705-715.
17. Hofmann K, Fiedler S, Vierkotten S, Weber J, Klee S, Jia J, Zwickenpflug W, Flockerzi V, Storch U, Yildirim AO, Gudermann T, Konigshoff M, Dietrich A. Classical transient receptor potential 6 (TRPC6) channels support myofibroblast differentiation and development of experimental pulmonary fibrosis. *Biochim Biophys Acta* 2017; 1863: 560-568.
18. Rahaman SO, Grove LM, Paruchuri S, Southern BD, Abraham S, Niese KA, Scheraga RG, Ghosh S, Thodeti CK, Zhang DX, Moran MM, Schilling WP, Tschumperlin DJ, Olman MA. TRPV4 mediates myofibroblast differentiation and pulmonary fibrosis in mice. *J Clin Invest* 2014; 124: 5225-5238.
19. Hu F, Song X, Long D. Transient receptor potential ankyrin 1 and calcium: Interactions and association with disease (Review). *Exp Ther Med* 2021; 22: 1462.

20. Kurahara LH, Hiraishi K, Hu Y, Koga K, Onitsuka M, Doi M, Aoyagi K, Takedatsu H, Kojima D, Fujihara Y, Jian Y, Inoue R. Activation of Myofibroblast TRPA1 by Steroids and Pirfenidone Ameliorates Fibrosis in Experimental Crohn's Disease. *Cell Mol Gastroenterol Hepatol* 2018; 5: 299-318.
21. Li W, Zhang Z, Li X, Cai J, Li D, Du J, Zhang B, Xiang D, Li N, Li Y. CGRP derived from cardiac fibroblasts is an endogenous suppressor of cardiac fibrosis. *Cardiovasc Res* 2020; 116: 1335-1348.
22. Webert L, Faro D, Zeitlmayr S, Gudermann T, Breit A. Analysis of the Glucose-Dependent Transcriptome in Murine Hypothalamic Cells. *Cells* 2022; 11.
23. Love MI, Huber W, Anders S. Moderated estimation of fold change and dispersion for RNA-seq data with DESeq2. *Genome biology* 2014; 15: 550.
24. Yu G, Wang LG, Han Y, He QY. clusterProfiler: an R package for comparing biological themes among gene clusters. *OMICS* 2012; 16: 284-287.
25. Wu SR, Lin CH, Shih HP, Ko CJ, Lin HY, Lan SW, Lin HH, Tu HF, Ho CC, Huang HP, Lee MS. HAI-2 as a novel inhibitor of plasmin represses lung cancer cell invasion and metastasis. *Br J Cancer* 2019; 120: 499-511.
26. Zeitlmayr S, Zierler S, Staab-Weijnitz CA, Dietrich A, Geiger F, Horgen FD, Gudermann T, Breit A. TRPM7 restrains plasmin activity and promotes transforming growth factor-beta1 signaling in primary human lung fibroblasts. *Archives of toxicology* 2022.
27. Zhou W, Pal AS, Hsu AY, Gurol T, Zhu X, Wirbisky-Hershberger SE, Freeman JL, Kasinski AL, Deng Q. MicroRNA-223 Suppresses the Canonical NF-kappaB Pathway in Basal Keratinocytes to Dampen Neutrophilic Inflammation. *Cell reports* 2018; 22: 1810-1823.
28. Dennler S, Itoh S, Vivien D, ten Dijke P, Huet S, Gauthier JM. Direct binding of Smad3 and Smad4 to critical TGF beta-inducible elements in the promoter of human plasminogen activator inhibitor-type 1 gene. *EMBO J* 1998; 17: 3091-3100.
29. Virk HS, Rekas MZ, Biddle MS, Wright AKA, Sousa J, Weston CA, Chachi L, Roach KM, Bradding P. Validation of antibodies for the specific detection of human TRPA1. *Scientific reports* 2019; 9: 18500.
30. Takaya J, Mio K, Shiraishi T, Kurokawa T, Otsuka S, Mori Y, Uesugi M. A Potent and Site-Selective Agonist of TRPA1. *Journal of the American Chemical Society* 2015; 137: 15859-15864.
31. Kretzschmar M, Doody J, Massague J. Opposing BMP and EGF signalling pathways converge on the TGF-beta family mediator Smad1. *Nature* 1997; 389: 618-622.
32. Kretzschmar M, Doody J, Timokhina I, Massague J. A mechanism of repression of TGFbeta/ Smad signaling by oncogenic Ras. *Genes Dev* 1999; 13: 804-816.
33. Dolivo DM, Larson SA, Dominko T. Crosstalk between mitogen-activated protein kinase inhibitors and transforming growth factor-beta signaling results in variable activation of human dermal fibroblasts. *Int J Mol Med* 2019; 43: 325-335.
34. Schaefer EA, Stohr S, Meister M, Aigner A, Gudermann T, Buech TR. Stimulation of the chemosensory TRPA1 cation channel by volatile toxic substances promotes cell survival of small cell lung cancer cells. *Biochem Pharmacol* 2013; 85: 426-438.
35. Kamato D, Do BH, Osman N, Ross BP, Mohamed R, Xu S, Little PJ. Smad linker region phosphorylation is a signalling pathway in its own right and not only a modulator of canonical TGF-beta signalling. *Cell Mol Life Sci* 2020; 77: 243-251.
36. Breton JD, Heydet D, Starrs LM, Veldre T, Ghildyal R. Molecular changes during TGFbeta-mediated lung fibroblast-myofibroblast differentiation: implication for glucocorticoid resistance. *Physiol Rep* 2018; 6: e13669.
37. Staab-Weijnitz CA, Fernandez IE, Knuppel L, Maul J, Heinzelmann K, Juan-Guardela BM, Hennen E, Preissler G, Winter H, Neurohr C, Hatz R, Lindner M, Behr J, Kaminski N, Eickelberg O. FK506-Binding Protein 10, a Potential Novel Drug Target for Idiopathic Pulmonary Fibrosis. *American journal of respiratory and critical care medicine* 2015; 192: 455-467.

38. Bendiks L, Geiger F, Gudermann T, Feske S, Dietrich A. Store-operated Ca(2+) entry in primary murine lung fibroblasts is independent of classical transient receptor potential (TRPC) channels and contributes to cell migration. *Scientific reports* 2020; 10: 6812.
39. Achanta S, Jordt SE. Transient receptor potential channels in pulmonary chemical injuries and as countermeasure targets. *Annals of the New York Academy of Sciences* 2020; 1480: 73-103.
40. Steinritz D, Stenger B, Dietrich A, Gudermann T, Popp T. TRPs in Tox: Involvement of Transient Receptor Potential-Channels in Chemical-Induced Organ Toxicity-A Structured Review. *Cells* 2018; 7.
41. Yap JMG, Ueda T, Kanemitsu Y, Takeda N, Fukumitsu K, Fukuda S, Uemura T, Tajiri T, Ohkubo H, Maeno K, Ito Y, Oguri T, Ugawa S, Niimi A. AITC inhibits fibroblast-myofibroblast transition via TRPA1-independent MAPK and NRF2/HO-1 pathways and reverses corticosteroids insensitivity in human lung fibroblasts. *Respiratory research* 2021; 22: 51.
42. Virk HS, Biddle MS, Smallwood DT, Weston CA, Castells E, Bowman VW, McCarthy J, Amrani Y, Duffy SM, Bradding P, Roach KM. TGFbeta1 induces resistance of human lung myofibroblasts to cell death via down-regulation of TRPA1 channels. *British journal of pharmacology* 2021; 178: 2948-2962.
43. Faouzi M, Penner R. Trpm2. *Handb Exp Pharmacol* 2014; 222: 403-426.
44. Samapati R, Yang Y, Yin J, Stoerger C, Arenz C, Dietrich A, Gudermann T, Adam D, Wu S, Freichel M, Flockerzi V, Uhlig S, Kuebler WM. Lung endothelial Ca2+ and permeability response to platelet-activating factor is mediated by acid sphingomyelinase and transient receptor potential classical 6. *American journal of respiratory and critical care medicine* 2012; 185: 160-170.
45. Pani B, Singh BB. Lipid rafts/caveolae as microdomains of calcium signaling. *Cell Calcium* 2009; 45: 625-633.
46. Henderson NC, Rieder F, Wynn TA. Fibrosis: from mechanisms to medicines. *Nature* 2020; 587: 555-566.

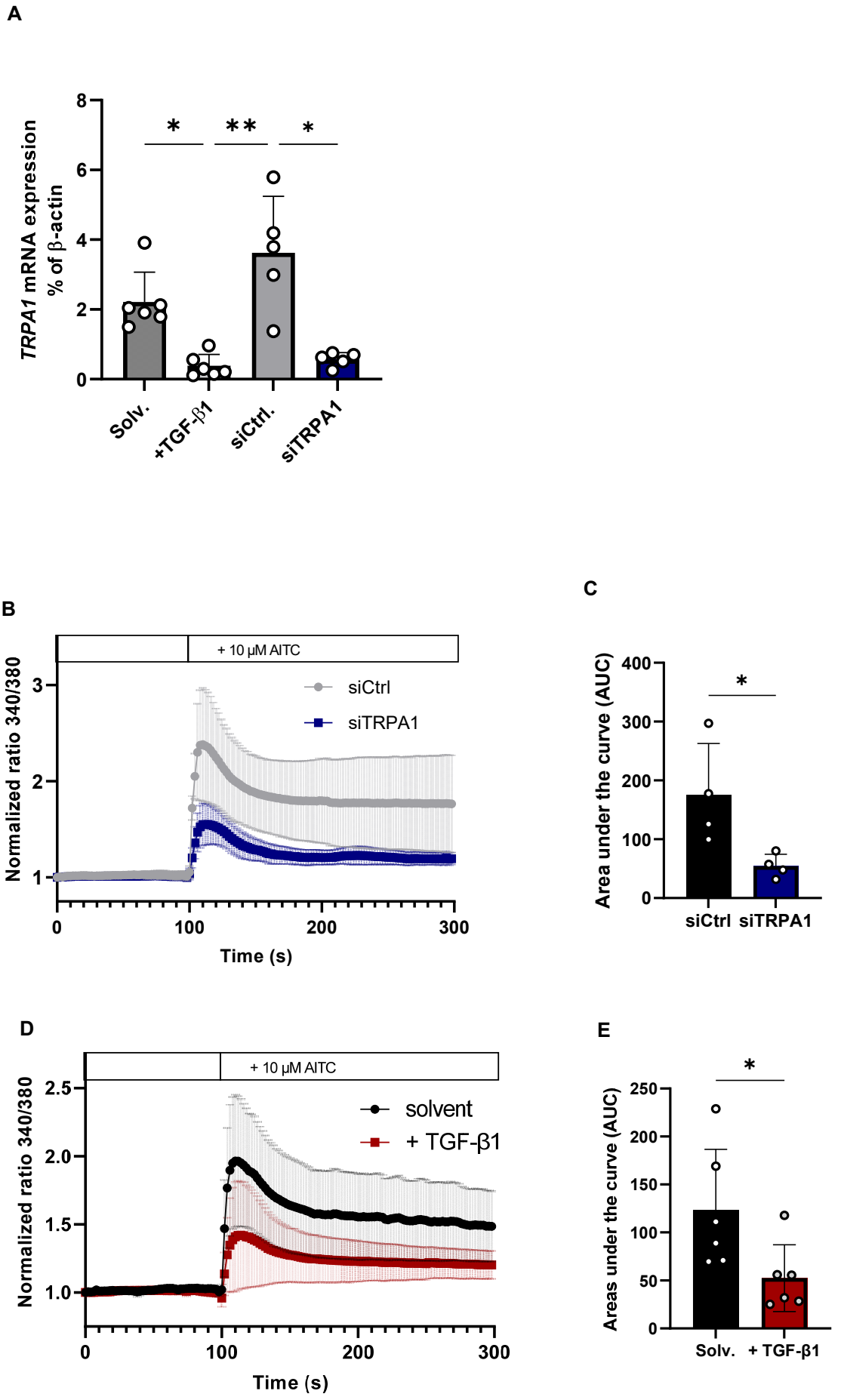
A
TRPA1 mRNA expression
% of β-actin
Solv.
+TGF-β1
siCtrl.
siTRPA1
B
+ 10 µM AITC
siCtrl
siTRPA1
Normalized ratio 340/380
Time (s)
C
Area under the curve (AUC)
siCtrl
siTRPA1
D
+ 10 µM AITC
solvent
+ TGF-β1
Normalized ratio 340/380
Time (s)
E
Areas under the curve (AUC)
Solv.
+ TGF-β1

Figure 1

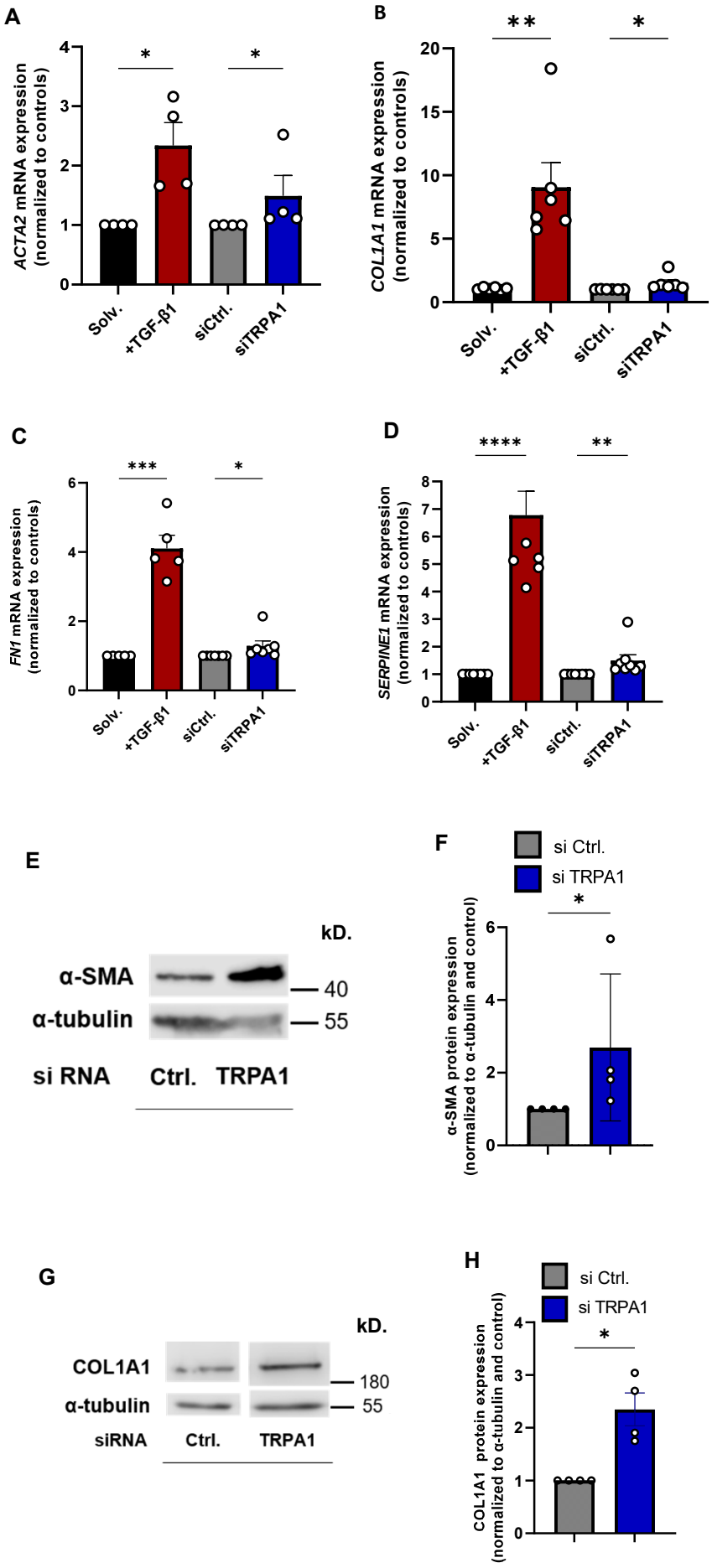
A
ACTA2 mRNA expression (normalized to controls)
Solv.
+TGF-β1
siCtrl.
siTRPA1
B
COL1A1 mRNA expression (normalized to controls)
C
FN1 mRNA expression (normalized to controls)
D
SERPINE1 mRNA expression (normalized to controls)
E
kD.
α-SMA
α-tubulin
40
55
si RNA
Ctrl.
TRPA1
F
si Ctrl.
si TRPA1
α-SMA protein expression (normalized to α-tubulin and control)
G
kD.
COL1A1
α-tubulin
180
55
siRNA
Ctrl.
TRPA1
H
si Ctrl.
si TRPA1
COL1A1 protein expression (normalized to α-tubulin and control)

Figure 2

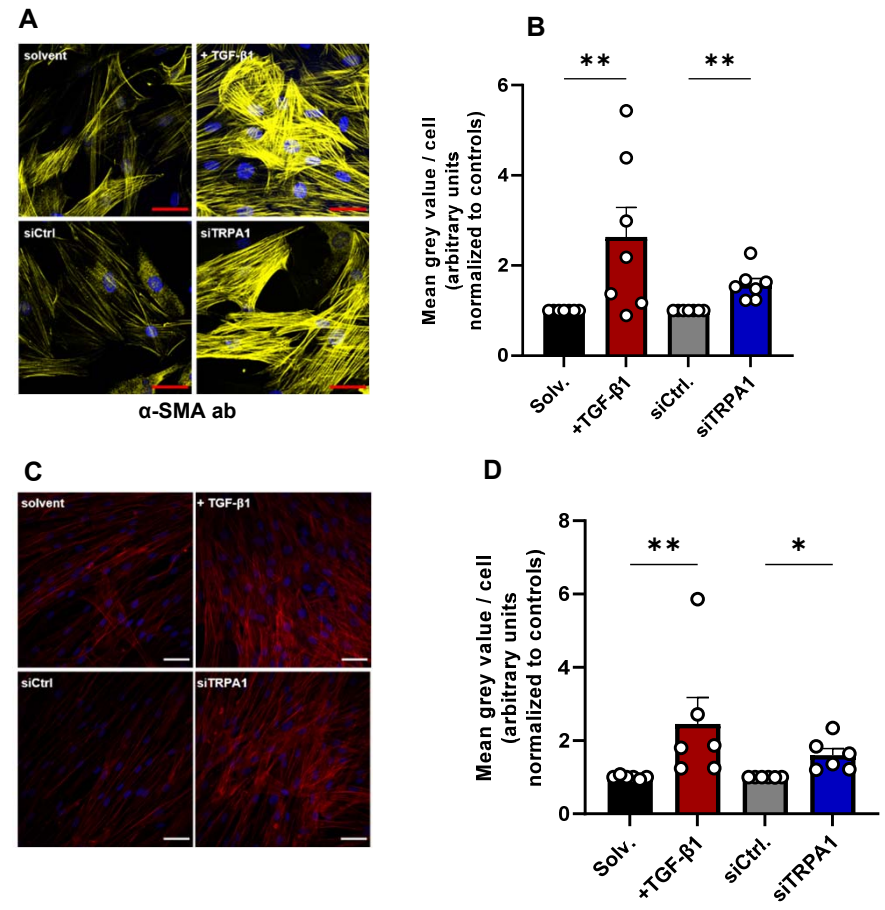
A
solvent
+TGF-β1
siCtrl
siTRPA1
α-SMA ab
B
Mean grey value / cell (arbitrary units normalized to controls)
Solv.
+TGF-β1
siCtrl.
siTRPA1
C
solvent
+ TGF-β1
siCtrl
siTRPA1
D
Mean grey value / cell (arbitrary units normalized to controls)
Solv.
+TGF-β1
siCtrl.
siTRPA1

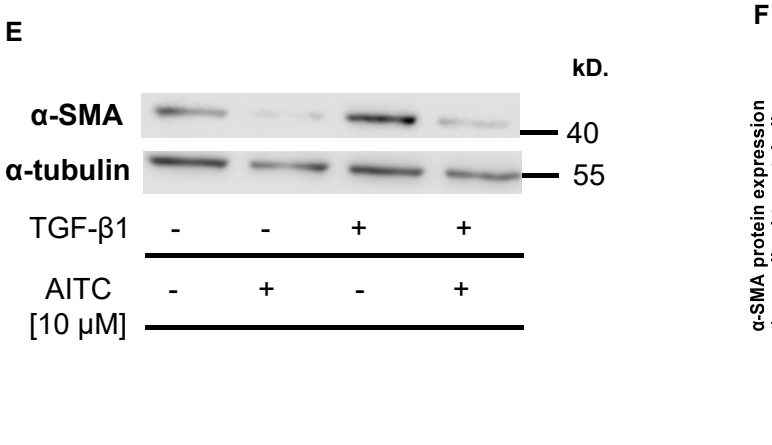
E
kD.
α-SMA
α-tubulin
40
55
TGF-β1
AITC [10 μM]

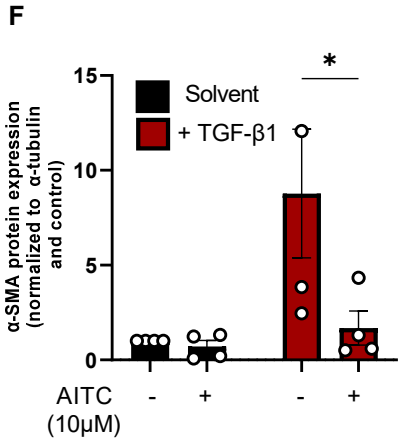
F
α-SMA protein expression (normalized to α-tubulin and control)
Solvent
+ TGF-β1
AITC (10μM)

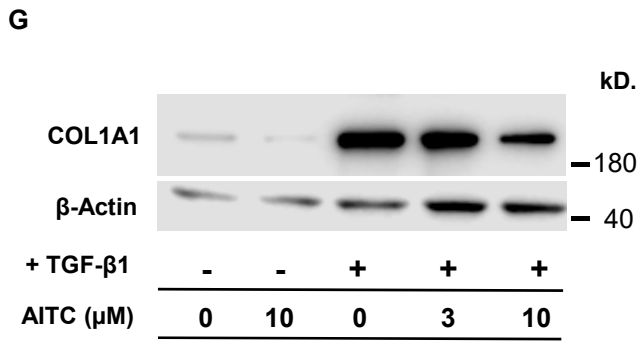
G
kD.
COL1A1
β-Actin
180
40
+ TGF-β1
AITC (μM)
0 10 0 3 10

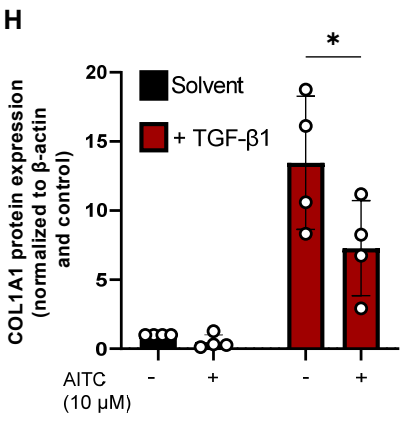
H
COL1A1 protein expression (normalized to β-actin and control)
Solvent
+ TGF-β1
AITC (10 μM)

Figure 3

A

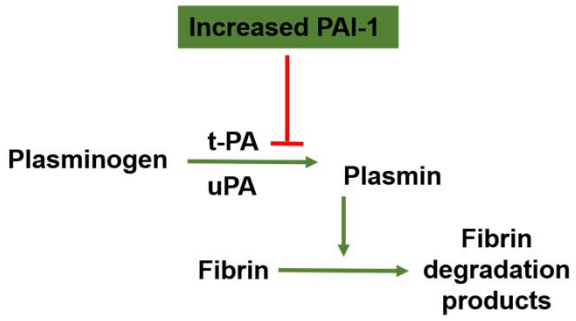

B

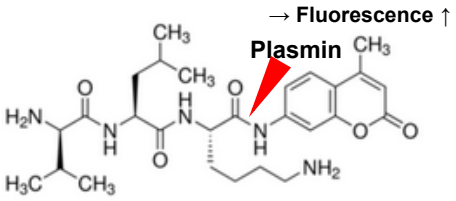

D-Val-Leu-Lys 7-amido-4-methylcoumarin
(D-VLK-AMC)

C

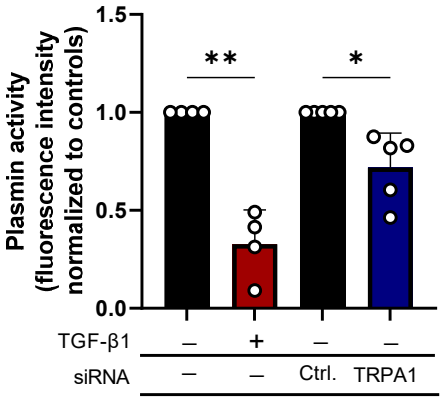

D

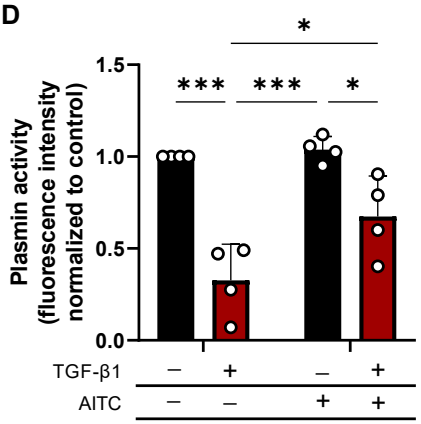

Figure 4

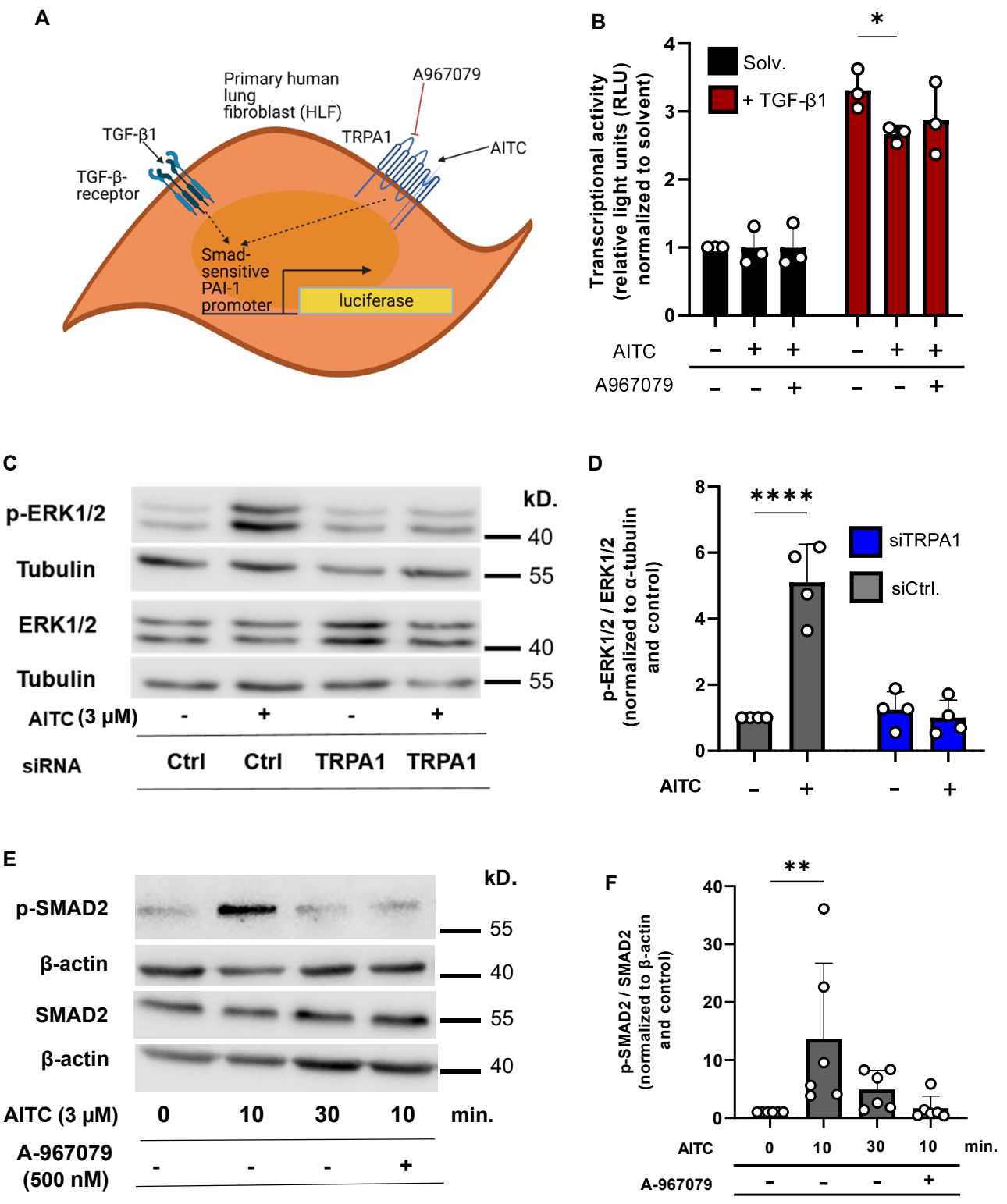
A
Primary human lung fibroblast (HLF)
A967079
TGF-β1
TRPA1
AITC
TGF-β-receptor
Smad-sensitive PAI-1 promoter
luciferase
B
Transcriptional activity (relative light units (RLU) normalized to solvent)
Solv.
+ TGF-β1
*
AITC
A967079
C
p-ERK1/2
Tubulin
ERK1/2
Tubulin
kD.
40
55
40
55
AITC (3 μM)
siRNA
Ctrl
Ctrl
TRPA1
TRPA1
D
p-ERK1/2 / ERK1/2 (normalized to α-tubulin and control)
****
siTRPA1
siCtrl.
AITC
E
p-SMAD2
β-actin
SMAD2
β-actin
kD.
55
40
55
40
AITC (3 μM)
0
10
30
10
min.
A-967079 (500 nM)
F
p-SMAD2 / SMAD2 (normalized to β-actin and control)
**
AITC
0
10
30
10
min.
A-967079

Figure 5

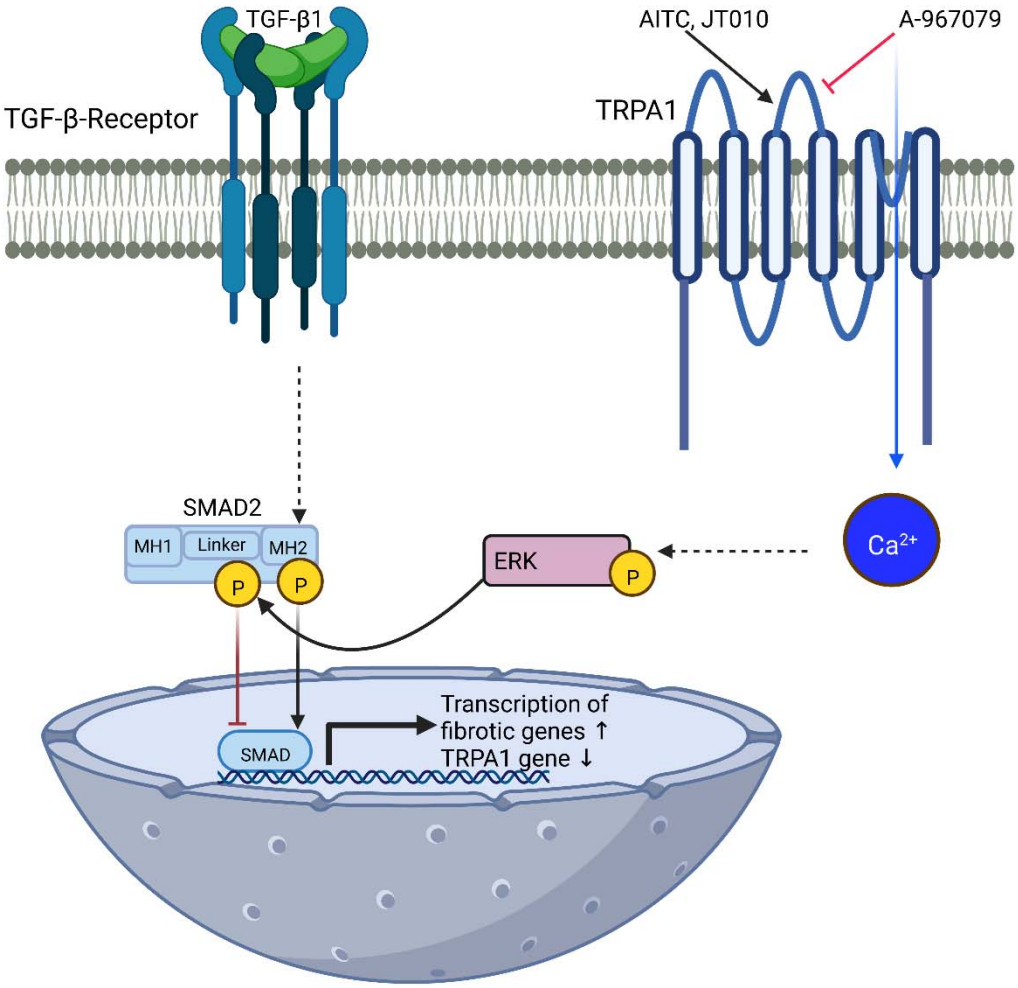
TGF-β1
TGF-β-Receptor
AITC, JT010
A-967079
TRPA1
SMAD2
MH1
Linker
MH2
P
P
ERK
P
Ca2+
SMAD
Transcription of
fibrotic genes ↑
TRPA1 gene ↓

Figure 6

An Inhibitory Function of TRPA1 Channels in TGF-β1-driven Fibroblast to Myofibroblast Differentiation

Fabienne Geiger[1], Sarah Zeitlmayr[1], Claudia A. Staab-Weijnitz[2], Suhasini Rajan[1], Andreas Breit[1], Thomas Gudermann[1], Alexander Dietrich[1]

[1] Walther Straub Institute of Pharmacology and Toxicology, Member of the German Center for Lung Research (DZL), LMU-Munich, Munich Germany.

[2] Comprehensive Pneumology Center with the CPC-M BioArchive and Institute of Lung Health and Immunity, Helmholtz-Zentrum München, Member of the German Center of Lung Research (DZL), Munich, Germany

Data Supplement

Supplementary Materials and Methods:

Cell culture

HLFs were grown in media containing 2 % (Lonza, #CC-3132; PromoCell, #C-23020) or 10 % (DZL (DMEM/F12, Lonza, #BE12-719F)) serum and seeded at a density of $3*10^5$ cells per well of a six well plate for experiments. On the next day, the medium was changed to starving conditions (0.1 % serum) or Accell siRNA delivery medium provided by the manufacturer (Dharmacon/HorizonDiscovery, Cambridge, UK, #B-005000-500) for 24 h, followed by rhTGF-β1 (bio-techne, Wiesbaden, Germany #240-B-002, 2 ng/ml) treatment for 48 h or siRNA knockdown (TRPA1 (#E-006109-00-0050)/scramble (#D-001910-10-50), 1 µM) for five days. A pool of four different TRPA1-specific siRNAs was used and siRNA transfection occurred without the use of transfection reagents by passive uptake of the siRNA. HLFs were pretreated with siRNA for three days and co-stimulated with siRNA and TGF-β1 for additional two days, if TGF-β1 treatment and TRPA1 knockdown were analyzed simultaneously. AITC (Sigma-Aldrich, Taufkirchen, Germany, #377430-5G, 3 µM or 10 µM as

indicated) and the TRPA1 inhibitor A-967079 (Sigma-Aldrich, #SML0085-5MG, 500 nM) were applied as indicated. For depletion of extracellular Ca^{2+}, the cell culture medium was exchanged to Hank's buffered saline solution (HBSS, Lonza, #BE10-527F). To remove extracellular Ca^{2+}, 2 mM ethylene glycol-bis(β-aminoethyl ether)-*N*,*N*,*N*′,*N*′-tetraacetic acid (EGTA, Roth, #3054.2) dissolved in H_2O adjusted to pH 8 with NaOH or H_2O (pH 8.0 adjusted with NaOH) was added and AITC was applied in the indicated concentrations immediately.

Quantitative Reverse-Transcription (qRT)-PCR

Total RNA from HLFs was isolated using the RNeasy Plus Mini Kit (Qiagen, Hilden, Germany, #74136). The mRNA (1 µg) was transcribed into first-strand cDNA using RevertAid H MINUS 1st cDNA KIT containing reverse transcription polymerase (Life Technologies, Darmstadt, Germany, #K1631) and random primer according to the manufactures instructions. mRNA levels of target genes were analyzed by real-time quantitative PCR as previously described (1). 2 µl of the cDNA was added to 8 µl of a master mix consisting of 2x ABsolute QPCR SYBR Green Mix (Life Technologies, #AB1158B), 10 pmol of each specific primer pair (see Table 1, Metabion, Planegg, Germany) and water. The following PCR program was run in a light-cycler apparatus (Roche, Mannheim, Germany): initial activation (15 min. at 94 °C) , 45 cycles of denaturation, annealing and extension (12 s at 94 °C, 30 s at 50 °C and 30 s at 72 °C) and melting curve determination to exclude samples that generated primer dimers or unspecific amplification products. The fluorescence intensities after each extension phase were measured, allowing the calculation of the crossing points (Cp) by the software (Roche, Basel, Switzerland, Light Cycler). Gene expression is shown in

relation to a housekeeping control gene (*ACTB*) and the relative expression was determined using 2-ΔΔCt.

Table 1: DNA-Sequences of qRT-PCR primers

Gene	Forward	Reverse
ANKTM1 (*TRPA1*) (2)	TCACCATGAGCTAGCAGACTATTT	GAGAGCGTCCTTCAGAATCG
ACTA2 (α-SMA)	GAC CCT GAA GTA CCC GAT AGA AC	GGG CAA CAC GAA GCT CAT TG
COL1A1	CAA GAG GAA GGC CAA GTC GAG	TTG TCG CAG ACG CAG ATC C
FN1	CCG ACC AGA AGTTTGGGT TCT	CAATGCGGT ACA TGACCC CT
SERPINE1 (PAI-1)	GAC ATC CTG GAA CTG CCC TA	GGT CAT GTT GCC TTT CCA GT
ACTB	CCA ACC GCG AGA AGA TGA	CCA GAG GCG TAC AGG GAT AG

Western Blot

Expression and phosphorylation of target proteins were evaluated by Western Blot analysis as previously described (1). HLFs were treated as described in section ”cells”, lysed with RIPA buffer (20 mM Tris-HCL, pH 7.5, 150 mM NaCl, 1 % Nonidet P40, 0.5 % sodium deoxycholate, 1 % SDS, 5 mM EDTA) containing phosphatase und protease inhibitors (Roche, Mannheim, Germany, #04906837001, #05892791001) for 30 min. on ice and sonicated for 15 s. The protein concentration was quantified using a Pierce™ BCA Protein Assay Kit (ThermoScientific, Rockford, US, #23225) following the manufacture’s protocol. The protein samples (10 µg protein and 1x Laemmli (5x buffer: 3 ml TRIS/HCL (2.6 M), pH 6.8; 10 ml glycerin; 2 g SDS; 2 mg bromophenol blue and 5 ml β-mercaptoethanol)) were heated for 10 min. at 95 °C and loaded onto a 10 % SDS PAGE. Gel electrophoreses was performed for 30 min. at 70 Volts followed by 1.5 h at 100 Volts at RT. The proteins were transferred to a Roti®-PVDF membrane (Roth, Karlsruhe, Germany, #T830.1) using a wet blot system (BioRad,

Feldkirchen, Germany) with a current of 250 mA for 1.5 h. The membrane was blocked with 5 % low fat milk (Roth, #T145.2) in TBS-T (0.1 %) for 1 h at RT. The antibodies were diluted in blocking solution and applied over night at 4 °C. HRP-conjugated secondary antibodies were applied for 2 h at RT. The chemiluminescence signal of the membranes was imaged after incubation in SuperSignal West Femto maximum sensitivity substrate (Life Technologies, #34095) with in an Odyssey-Fc-unit (Licor, Lincoln, NE, USA). Used antibodies and dilutions: p44/42 MAPK (ERK1/2) (Cell Signaling, #4695S, 1:1,000), Phospho-p44/42 MAPK (ERK1/2) (Thr202/Tyr204) (Cell Signaling, #4370S, 1:1,000), MAPK p38 (Cell Signaling #9212, 1:1000), pMAPK p38 (Cell Signaling #4511, 1:1000), α-smooth muscle actin (Sigma-Aldrich, #A5228, 1:2,000), Collagen1A1 (CellSignaling, #72026, 1:1,000), SMAD2 (CellSignaling, #3103 1:1,000), Phospho-SMAD2 (Ser245/250/255) (CellSignaling, #3104 1:1,000), β-actin-HRP (Sigma-Aldrich, #A3854, 1:10,000), α-tubulin (Abcam, #ab4074, 1:2,000), secondary anti-rabbit IgG peroxidase (POX)-antibody (Sigma-Aldrich, #A6154, 1:10,000), secondary anti-mouse IgG-HRP (CellSignaling, #7076S, 1:2,000).

~~**Electric cell-substrate impedance sensing (ECIS)**~~

~~The barrier function of cells can be quantified using electric cell-substrate impedance sensing (ECIS). After coating (L-Cysteine (10 mM, 10 min., RT) and FCS (overnight, 37 °C, 5 % CO_2)), HLFs were seeded at a density of 10,000 cells per well of a slide (ibidi, Gräfelfing, Germany, #8W10E+). A frequency of 8,000 Hz was applied and the cellular resistance was measured every two min. using an ECIS ZΘ (Applied Biophysics, Troy, NY, USA). Starving, TGF-β1/siRNA treatment and AITC stimulation were performed as mentioned above.~~

Water Soluble Tetrazolium (WST) Assay

To assess the cell viability of fibrotic and non-fibrotic fibroblasts after TRPA1 activation by AITC (3 µM, 24 h), HLFs were seeded at a density of 5,000 per well of a 24-well plate and treated. The cell culture media was aspirated, 500 µl of the cell proliferation WST-1 reagent (Sigma-Aldrich, #11644807001, 1:100 in medium,) was added to each well and incubated (37 °C, 5 % CO2, 3 h). The optical densities were measured in clear 96-well plates (100 µl/well in triplicates) using a plate reader (Tecan, Infinite M200 Pro).

Caspase Assay

Cell apoptosis was analyzed with the help of a CASPASE 3/7 Glo Assay (Promega, Walldorf, Germany, #G8091). HLFs were seeded at a density of 1,800 cells per well in a flat bottom white 96-well plate. siRNA (5 day), TGF-β1 (48 h) and AITC (24 h) treatment is described above. The assay was performed according to the manufactures protocol. In short, the appropriate amount of Caspase Glow reagent was added to the cells, media and reagent was thoroughly mixed (30 s, 300 rpm) and the assay was incubated for 1 h at RT. Luminescence was measured with a plate reader (Tecan, Infinite M200 Pro).

Calcium Imaging

TGF-β1/solvent or siRNA treated HLFs, which were grown on 25 mm coverslips until 80 % confluence, were loaded with Fura-2-AM (2 µM, Sigma-Aldrich, Taufkirchen, Germany, #47989-1MG-F) in Ca^{2+}-buffer (0.1 % BSA in HBSS (with Ca^{2+}, Mg^{2+})/HEPES (0.5 M)) at RT for 30 min. HLFs were washed with Ca^{2+}-buffer and placed on the 40x oil-objective of a Leica DMi8 fluorescence microscope in a quick change chamber (Warner instruments, Holliston, USA, #64-0367) covered with 400/450 µl Ca^{2+}-buffer. The change of the intracellular calcium concentration after application of the specific TRPA1 agonists AITC (10 µM/3 µM) or JT010 (75 nM)

with/out pre-blocking of the channel with A-967079 (500 nM) was measured at 340 and 380 nm as described (1).

Immunofluorescence

The cells were grown on 10 mm coverslips (three per six well) and treated as described in the section “cells” above. The HLFs were washed with PBS (Sigma-Aldrich, #D8537), fixed with 4 % PFA (Merck Millipore, Darmstadt, Germany, #104003) for 10 min at RT, permeabilized (0.5 % Triton X-100, 10 min, RT) and blocked with 4 % goat serum in 4 % BSA/PBS (1 h, RT). The primary antibody was applied over night at 4 °C in a wet chamber. The secondary antibodies were applied for 2 h at RT. Afterwards the cells were washed and the nuclei were stained using Hoechst (ThermoScientific, #62249, 2 µg/ml, 10 min, RT). The cover slips were fixed on glass slides using DAKO Fluorescence mounting medium (Agilent Technologies, Glostrup, Denmark, #S3023). Images were acquired at λex 488 nm; λem 525 nm with a confocal scanning microscope (LSM 880, Carl Zeiss). Antibodies and dilutions: αSMA (Sigma-Aldrich, #A5228, 1:2,000), Fibronectin (Abcam, #ab2413, 1:200), secondary anti-mouse IgG-FITC (Sigma-Aldrich, #F9006, 1:80), secondary anti-rabbit IgG-Alexa Fluor 488 (Invitrogen, #A11008, 1:500).

For the Phalloidin (Sigma-Aldrich, P1951) staining, the cells were treated as previously mentioned. Phalloidin was applied at a concentration of 50 µg/ml for 40 min at RT. The coverslips were mounted to the glass slides and images were taken at λex 540-545 nm; λem 570-573 nm using a confocal scanning microscope (LSM 880, Carl Zeiss). Image analysis was performed with the ImageJ-Fiji software calculating the mean grey values of the cells.

References

1. Hofmann K, Fiedler S, Vierkotten S, Weber J, Klee S, Jia J, Zwickenpflug W, Flockerzi V, Storch U, Yildirim AO, Gudermann T, Konigshoff M, Dietrich A. Classical transient receptor potential 6 (TRPC6) channels support myofibroblast differentiation and development of experimental pulmonary fibrosis. *Biochim Biophys Acta* 2017; 1863: 560-568.
2. Hutchinson NX, Gibbs A, Tonks A, Hope-Gill BD. Airway expression of Transient Receptor Potential (TRP) Vanniloid-1 and Ankyrin-1 channels is not increased in patients with Idiopathic Pulmonary Fibrosis. *PLoS One* 2017; 12: e0187847.

Supplementary Figures:

Supplementary Figure Legends:

Figure E1: Transcriptomic analysis of primary human lung fibroblasts (HLFs) after application of TGF-β1 or solvent. (*A*) Volcano plot of differentially expressed genes in TGF-β1 treated HLF Significantly up- (green color) or down-regulated red color) as well as fibrotic marker genes are marked: *ACTA2*, α-smooth muscle actin; *COL1A1*, collagen 1A1; *FN1*, fibronectin-1; *SERPINE1*, plasminogen activator inhibitor 1. (*B*) Significantly up-regulated gene ontology (GO) biological processes after application of TGF-β1. Adjusted *P*-values (p-adjust) are color-coded from blue to red in increasing order. Normalized counts of *TRPC* genes (*C*), *TRPM* genes (*D*) *TRPV* genes (*E*) and the *TRPA1* gene (*F*) in human fibroblasts after application of solvent (black bars) or TGF-β1 (red bars). Normalized counts were generated using DESeq2 in R (n = 3 independent cell isolations each). Data were analyzed by a Kruskal-Wallis (*C*-*E*) or a Mann-Whitney test (*F*) and are presented as mean ± SEM (n = 3).

Figure E2: Evaluation of the specificity of commercially available antibodies directed against the TRPA1 protein in HEK293 cell line stably expressing TRPA1 channels. (*A*) A representative Ca^{2+} imaging experiment showing elevations of the intracellular Ca^{2+} concentrations quantified as normalized ratios 340/380 nm after adding the TRPA1 activator AITC (10 µM) to HEK293 cells stably expressing TRPA1 protein (HEK-

TRPA1) or HEK293 control cells (HEK) as described in the Data Supplement. Light grey areas represent SEM. (*B*) Areas under the curves were calculated and plotted as bars (green bars, HEK-TRPA1; black bars HEK). (*C*-*E*) Lysates from HEK293 control cells (HEK) and HEK cells stably expressing TRPA1 protein (HEK-TRPA1) were incubated in Western Blots with commercially available antibodies as described in the Data Supplement (*C*) TRPA1 (Thermo-Fisher Scientific, #PA5-22833, lot RH2256214, 1:400), (*D*) TRPA1 (Merck Millipore, #ST1685, lot J8261-6G8 1:200), (*E*) TRPA1 (Santa Cruz Biotechnology, #sc-376495, lot C2621, 1:100), (*F*) TRPA1 (Alomone labs, #ACC-037, lot ACC037AN2025, 1:1000). Beta-actin served as loading control. Data were analyzed by a Kruskal-Wallis test (*B*) and are presented as mean ± SEM (n = 3 independent experiments in B). For B, *P < 0.05 versus the value in HEK control cells.

Figure E3: Ca^{2+} imaging in primary human lung fibroblasts (HLFs) treated with the TRPA1 channel inhibitor A-967079. (*A*) HLFs were cultured with solvent (Solv.) or TGF-β1 (TGF-β1) and analyzed in Ca^{2+} imaging experiments as described in Materials and Methods. Cells were stimulated with JT010 (75 nM) at the indicated time point. Light colored areas represent SEM. (*B*) Areas under the curves were calculated and plotted as bars (JT010, Solv., black bar; JT010, TGF-β1, red bar). (*C*) HLFs were cultured with solvent (Solv.) or TGF-β1 (TGF-β1) and analyzed in Ca^{2+} imaging experiments as described in Materials and Methods. Cells were treated with A-967079 (500 nM) or solvent for 2 min. and stimulated with AITC (3 µM) at the indicated time points. Light colored areas represent SEM. (*D*) Areas under the curves were calculated and plotted as bars (Solv., grey bar; + TGF-β1, red bar). AITC and A-967079 (+) or solvent (-) were added as indicated. Data were analyzed by a Mann-Whitney test (*B*) or one-way ANOVA (*D*) and are presented as mean ± SEM (n = 5 independent experiments each in A-D). For B, *P < 0.05, **P < 0.01,***P < 0.001, ****P <0.0001 versus the value in cells treated with solvent alone.

Figure E4: Quantification of transcription and expression of fibrotic marker proteins in human lung fibroblasts (HLFs) cultured with or without TGF-β1. (*A, B*) Summaries of quantifications of α-smooth muscle actin (αSMA) (*A*) and collagen1A1 (COL1A) (*B*) protein levels in HLFs cultured with TGF-β1 and transfected with TRPA1 specific siRNAs (siRNA TRPA1) or scrambled siRNAs (siRNA Ctrl.). (*C*) α-smooth muscle actin (α-SMA) protein expression was quantified by Western blotting using a specific antiserum in HLFs cultured with or without TGF-β1 and/or treated with the TRPA1 activator JT010. Alpha-tubulin served as loading control. (*D*) Summary of α-SMA protein expression normalized to α-tubulin in HLFs cultured with or without TGF-β1 and/or treated with the TRPA1 activator JT010. (*E*) Collagen1A1 (COL1A1) protein expression was quantified by Western blotting using a specific antiserum in HLFs cultured with or without TGF-β1 and/or treated with the TRPA1 activator JT010. Alpha-tubulin served as loading control. (*F*) Summary of COL1A1 protein expression normalized to α-tubulin in HLFs cultured with or without TGF-β1 and/or treated with the TRPA1 activator JT010. (*G*) Indirect quantification of expression of plasminogen-activator-inhibitor 1 (PAI-1) activity in human lung fibroblasts (HLFs) cultured with (+) or without (-) TGF-β1 or treated with (+) or without (-) the TRPA1-specific activator AITC. Data were analyzed by a Mann-Whitney test (*A, B*) or two-way ANOVA (*D, F, G*) and are presented as mean ± SEM (n = 3 – 5 independent cell isolations each). For A, B, D, F, G *P < 0.05, ****P <0.0001 versus the value in cells treated with solvent alone.

Figure E5: Identification of MAPK p38 protein involved in TRPA1-mediated inhibition of TGF-β1-induced transcription. (*A*) Lysates from fibroblasts transfected with TRPA1

specific (siRNA TRPA1) or scrambled siRNA (siRNA Ctrl.) and treated with (+) or without (-) AITC were incubated in a Western Blot of with specific antibodies directed against phosphorylated MAPK p38 (p-MAPK p38) and MAPK p38 (MAPK p38). Alpha-tubulin served as loading control. (*B*) Summary of the p-MAPK p38/MAPK p38 quantification normalized to α-tubulin by Western Blotting in HLFs transfected with TRPA1 specific siRNAs (siTRPA1, blue bars) or scrambled siRNAs (siCtrl., grey bars) incubated with (+) or without (-) AITC. (*C*) Lysates from fibroblasts pretreated with TGF-β1, transfected with TRPA1 specific (siRNA TRPA1) or scrambled siRNA (siRNA Ctrl.) and incubated with (+) or without (-) AITC were incubated in a Western Blot of with specific antibodies directed against phosphorylated MAPK p38 (p-MAPK p38) and MAPK p38 (MAPK p38). Alpha-tubulin served as loading control. (*D*) Summary of the p-MAPK p38/MAPK p38 quantification normalized to α-tubulin by Western Blotting in HLFs pretreated with TGF-β1, transfected with TRPA1 specific siRNAs (siTRPA1, blue bars) or scrambled siRNAs (siCtrl., grey bars) and incubated with (+) or without (-) AITC. (*E*) Lysates from fibroblasts pretreated with TGF-β1, transfected with TRPA1 specific (siRNA TRPA1) or scrambled siRNA (siRNA Ctrl.) and incubated with (+) or without (-) AITC were incubated in a Western Blot of with specific antibodies directed against phosphorylated ERK1/2 (p-ERK1/2) and ERK1/2 (ERK1/2). Alpha-tubulin served as loading control. (*F*) Summary of the p-ERK1/2/ERK1/2 quantification normalized to α-tubulin and control by Western Blotting in HLFs pretreated with TGF-β1, transfected with TRPA1 specific siRNAs (siTRPA1, blue bars) or scrambled siRNAs (siCtrl., grey bars) and incubated with (+) or without (-) AITC. Data were analyzed by two-way ANOVA and are presented as mean ± SEM. Cells are from at least three independent donors and number of experiments is n = 4. **P < 0.01 versus the value in cells treated with solvent alone.

Figure E6: Ca^{2+}-dependency of AITC-induced ERK1/2 and MAPK p38 protein phosphorylation. (*A*) Lysates from fibroblasts treated with (+) or without (-) AITC in HBSS medium containing Ca^{2+} or EGTA (2mM) were incubated in a Western Blot with specific antibodies directed against phosphorylated ERK1/2 (p-ERK1/2) and ERK1/2. Alpha-tubulin served as loading control. (*B*) Summary of the p-ERK1/2/ERK1/2 quantification normalized to α-tubulin by Western Blotting in HLFs treated with (+) or without (-) AITC in HBSS medium containing Ca^{2+} (Ca^{2+}) or EGTA (EGTA). (*C*) Lysates from fibroblasts treated with (+) or without (-) AITC in HBSS medium containing Ca^{2+} or EGTA (2mM) were incubated in a Western Blot with specific antibodies directed against phosphorylated MAPK p38 (p-MAPK p38) and MAPK p38 (MAPK p38). Alpha-tubulin served as loading control. (*D*) Summary of the p-MAPK p38/MAPK p38 quantification normalized to α-tubulin by Western Blotting in HLFs treated with (+) or without (-) AITC in HBSS medium containing Ca^{2+} (Ca^{2+}) or EGTA (EGTA). Data were analyzed by two-way ANOVA and are presented as mean ± SEM. Cells are from three independent donors (n=3). **P < 0.01, ****P < 0.0001 versus the value in cells treated with solvent alone.

Figure E7: Identification of proteins involved in TRPA1-mediated inhibition of TGF-β1-induced transcription. (*A*) Summary of the p-SMAD2/SMAD2 quantification normalized to β-actin and control by Western Blotting in HLFs pretreated with TGF-β1, with (+) or without (-) A-967079 and incubated with (+) or without (-) AITC. (*B*) Lysates from fibroblasts treated with (+) or without (-) AITC in HBSS medium containing Ca^{2+} or EGTA (2mM) were incubated in a Western Blot with specific antibodies directed against phosphorylated SMAD2 (p-SMAD2) and SMAD2. B-actin served as loading control. (*C*) Summary of the p-SMAD2/SMAD2 quantification normalized to β-actin by Western Blotting in HLFs treated with (+) or without (-) AITC in HBSS medium containing Ca^{2+} (Ca^{2+}) or EGTA (EGTA). (*D*) Detection of SMAD3 protein in the

cytoplasmic fraction of HLFs pretreated with (+) or without (-) TGF-β1 and incubated with AITC for 0, 10 or 30 minutes. (*E*) Summary of SMAD3 protein quantifications in HLFs pretreated with (+) or without (-) TGF-β1 and incubated with AITC for 10 minutes. Data were analyzed by a Kruskal-Wallis test (*A*) or two-way ANOVA (*C, E*) and are presented as mean ± SEM. *P < 0.05 versus the value in cells treated with solvent alone.

Figure E8: Quantification of apoptosis and cell viability in human lung fibroblasts (HLFs). (*A*) HLFs cultured with solvent or TGF-β1 and transfected with a TRPA1-specific siRNA (siTRPA1) or a scrambled siRNA (siCtrl.) were incubated with the solvent (DMSO), AITC (AITC 3 µM or 6 µM) or tamoxifen (TAM) as positive control. Caspase 3 activity was detected as described in the Data Supplement. (*B*) HLFs cultured with solvent or TGF-β1 and transfected with a TRPA1-specific siRNA (siTRPA1) or a scrambled siRNA (siCtrl.) were incubated with the solvent (DMSO) or AITC for 2 or 24 h. WST assays were performed as described in the Data Supplement. Data were analyzed by two-way ANOVA and are presented as mean ± SEM (n = 3 independent cell isolations each in A-B). For A, ****P <0.0001 versus the value in cells treated with AITC or DMSO alone.

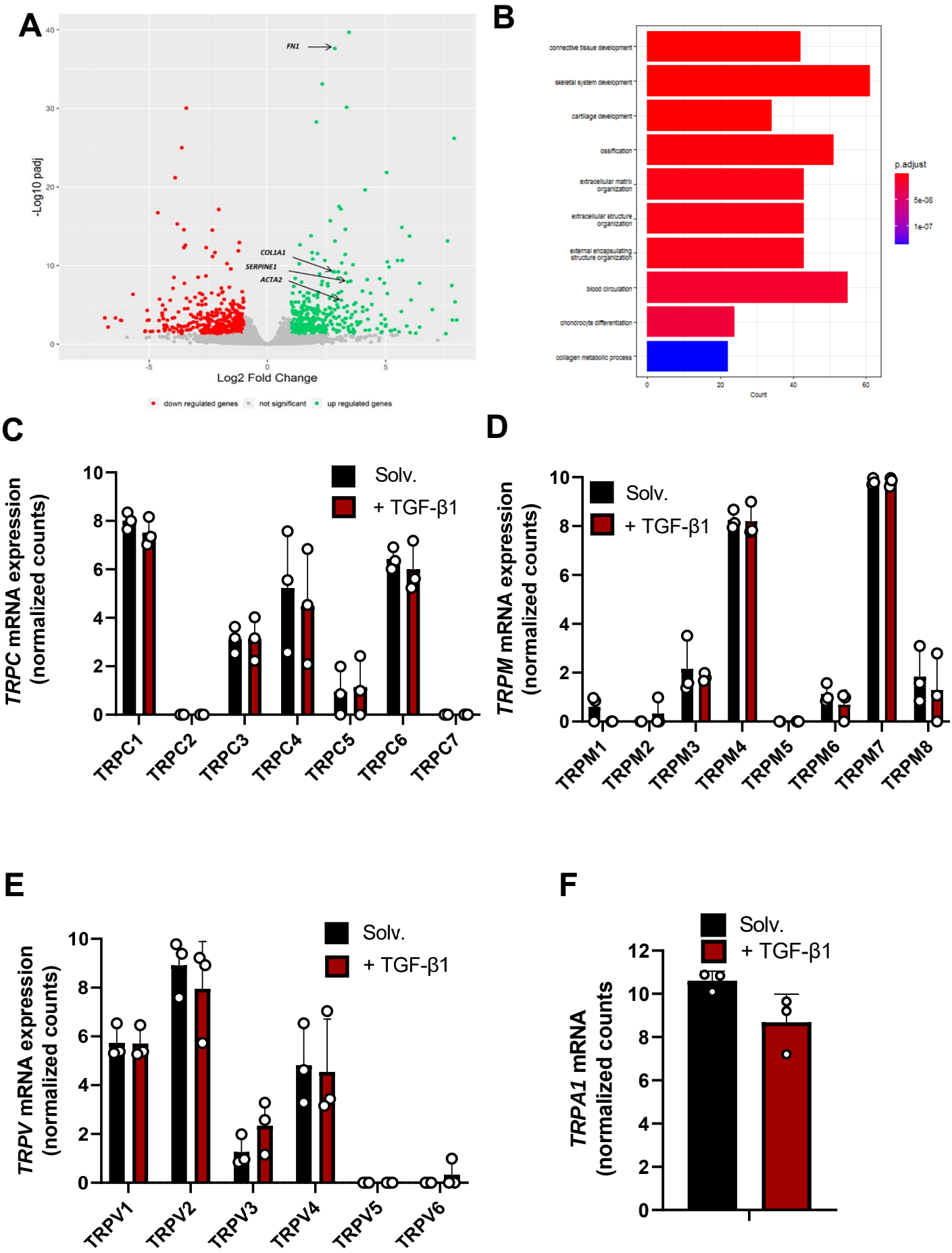
A
FN1
COL1A1
SERPINE1
ACTA2
-Log10 padj
Log2 Fold Change
down regulated genes
not significant
up regulated genes
B
connective tissue development
skeletal system development
cartilage development
ossification
extracellular matrix organization
extracellular structure organization
external encapsulating structure organization
blood circulation
chondrocyte differentiation
collagen metabolic process
p.adjust
5e-08
1e-07
Count
C
TRPC mRNA expression (normalized counts)
Solv.
+ TGF-β1
TRPC1
TRPC2
TRPC3
TRPC4
TRPC5
TRPC6
TRPC7
D
TRPM mRNA expression (normalized counts)
Solv.
+ TGF-β1
TRPM1
TRPM2
TRPM3
TRPM4
TRPM5
TRPM6
TRPM7
TRPM8
E
TRPV mRNA expression (normalized counts)
Solv.
+ TGF-β1
TRPV1
TRPV2
TRPV3
TRPV4
TRPV5
TRPV6
F
TRPA1 mRNA (normalized counts
Solv.
+ TGF-β1

Figure E1

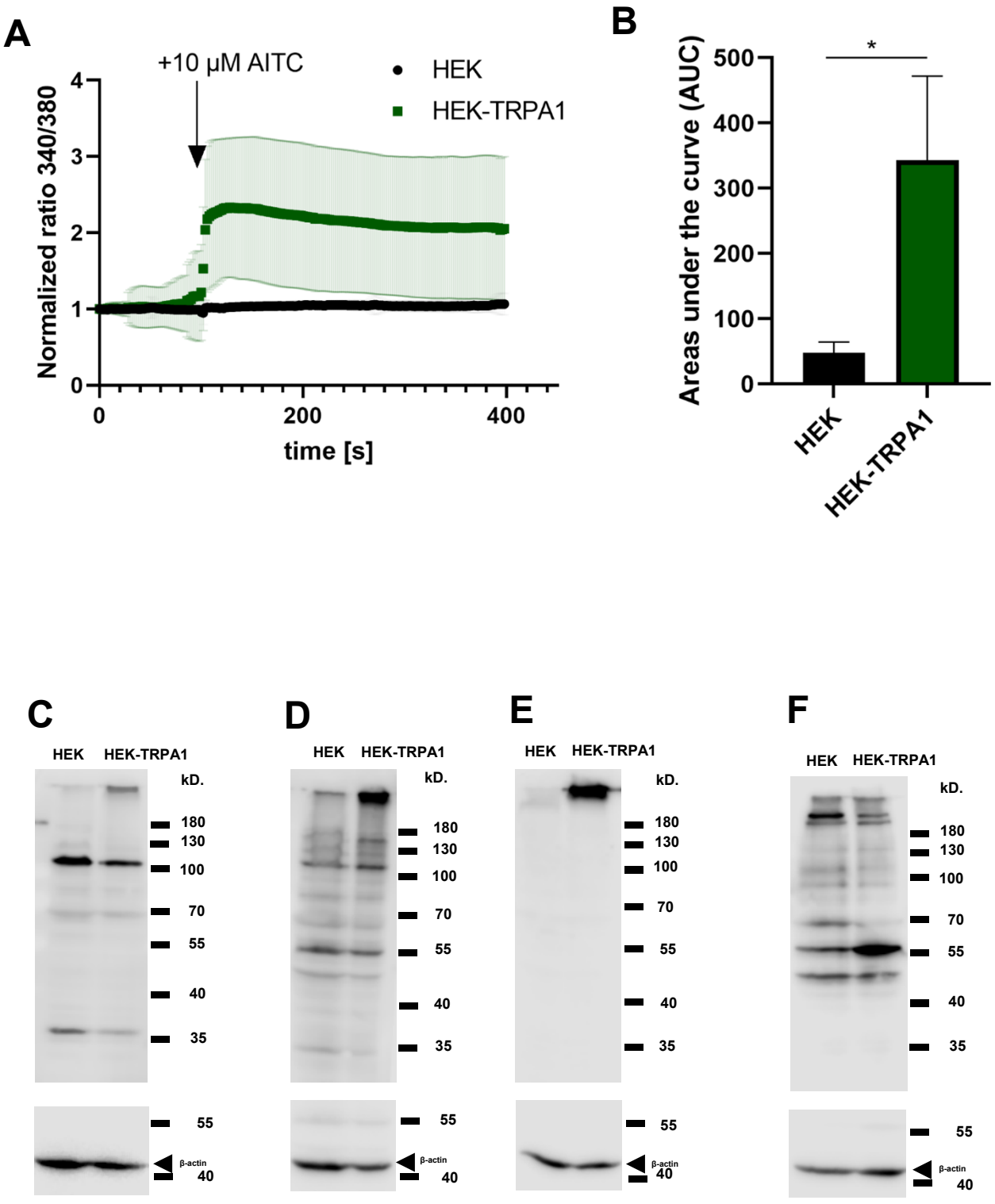
A
+10 µM AITC
HEK
HEK-TRPA1
Normalized ratio 340/380
time [s]
B
Areas under the curve (AUC)
*
HEK
HEK-TRPA1
C
D
E
F
HEK
HEK-TRPA1
kD.
180
130
100
70
55
40
35
β-actin

Figure E2

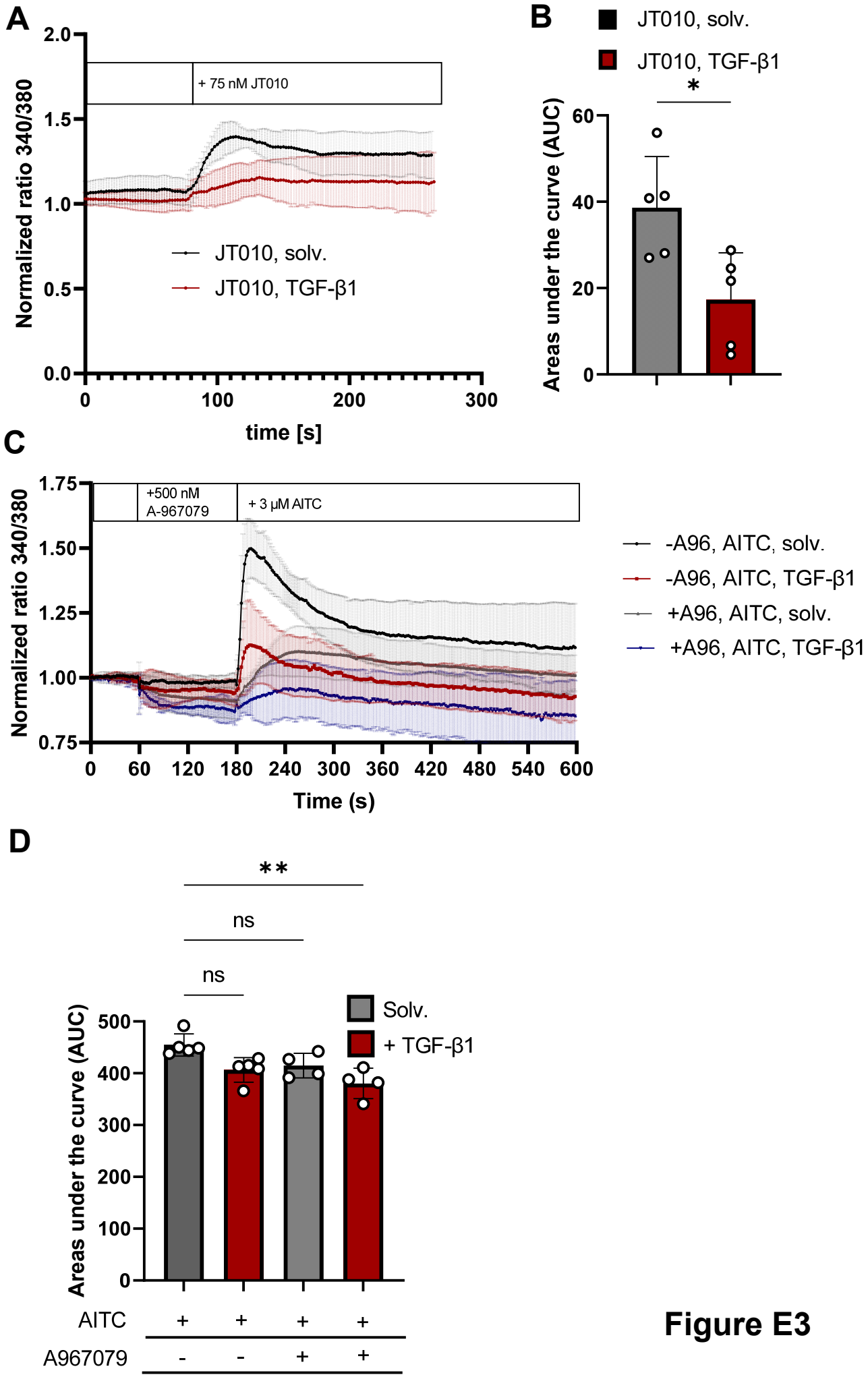
A
Normalized ratio 340/380
+ 75 nM JT010
JT010, solv.
JT010, TGF-β1
time [s]
B
JT010, solv.
JT010, TGF-β1
*
Areas under the curve (AUC)
C
Normalized ratio 340/380
+500 nM A-967079
+ 3 µM AITC
-A96, AITC, solv.
-A96, AITC, TGF-β1
+A96, AITC, solv.
+A96, AITC, TGF-β1
Time (s)
D
**
ns
ns
Solv.
+ TGF-β1
Areas under the curve (AUC)
AITC
A967079

Figure E3

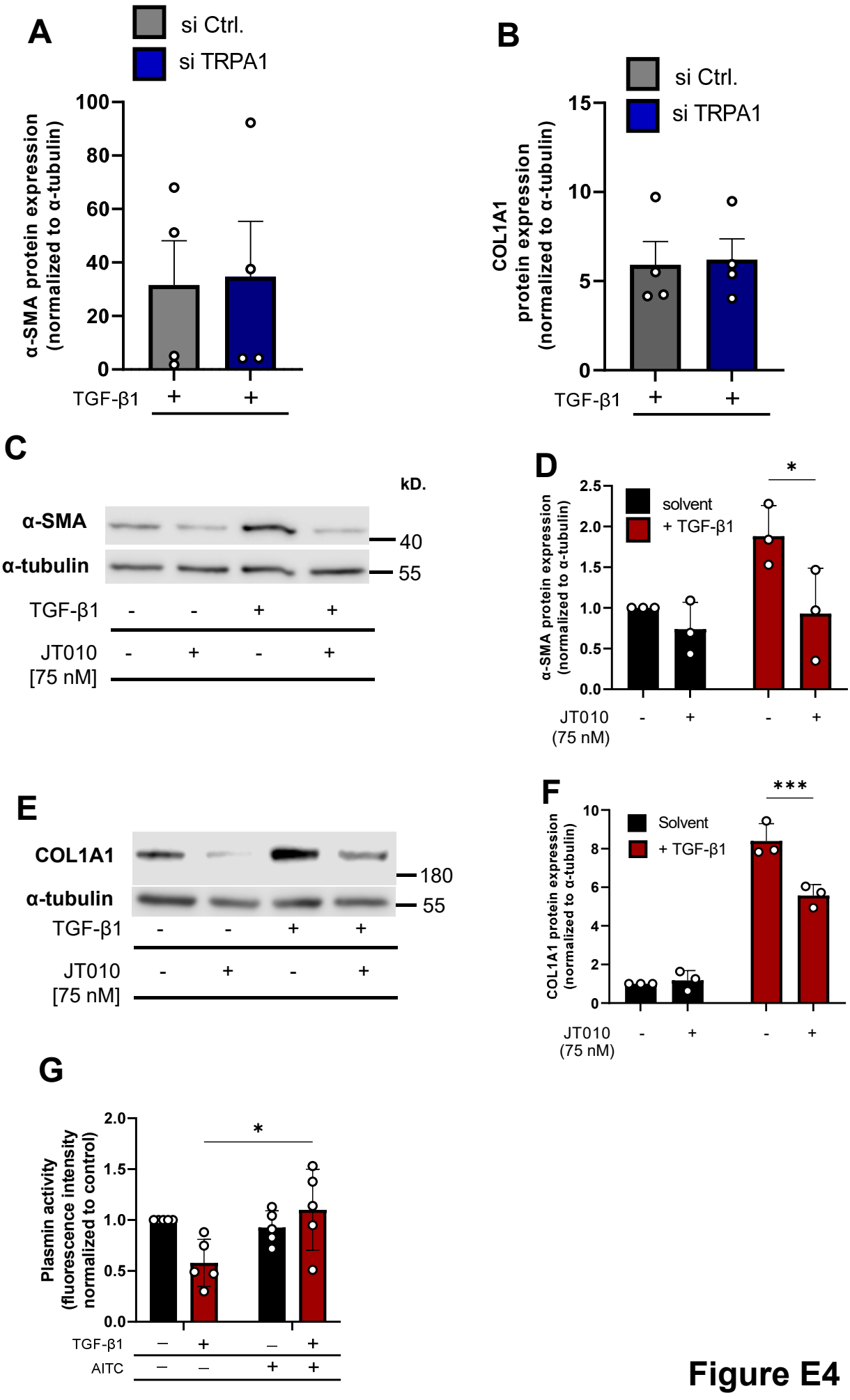
A
si Ctrl.
si TRPA1
α-SMA protein expression (normalized to α-tubulin)
100
80
60
40
20
0
TGF-β1 + +
B
si Ctrl.
si TRPA1
COL1A1 protein expression (normalized to α-tubulin)
15
10
5
0
TGF-β1 + +
C
kD.
α-SMA
α-tubulin
40
55
TGF-β1 - - + +
JT010 [75 nM] - + - +
D
solvent
+ TGF-β1
α-SMA protein expression (normalized to α-tubulin)
2.5
2.0
1.5
1.0
0.5
0.0
*
JT010 (75 nM) - + - +
E
COL1A1
α-tubulin
180
55
TGF-β1 - - + +
JT010 [75 nM] - + - +
F
Solvent
+ TGF-β1
COL1A1 protein expression (normalized to α-tubulin)
10
8
6
4
2
0
***
JT010 (75 nM) - + - +
G
Plasmin activity (fluorescence intensity normalized to control)
2.0
1.5
1.0
0.5
0.0
*
TGF-β1 – + – +
AITC – – + +

Figure E4

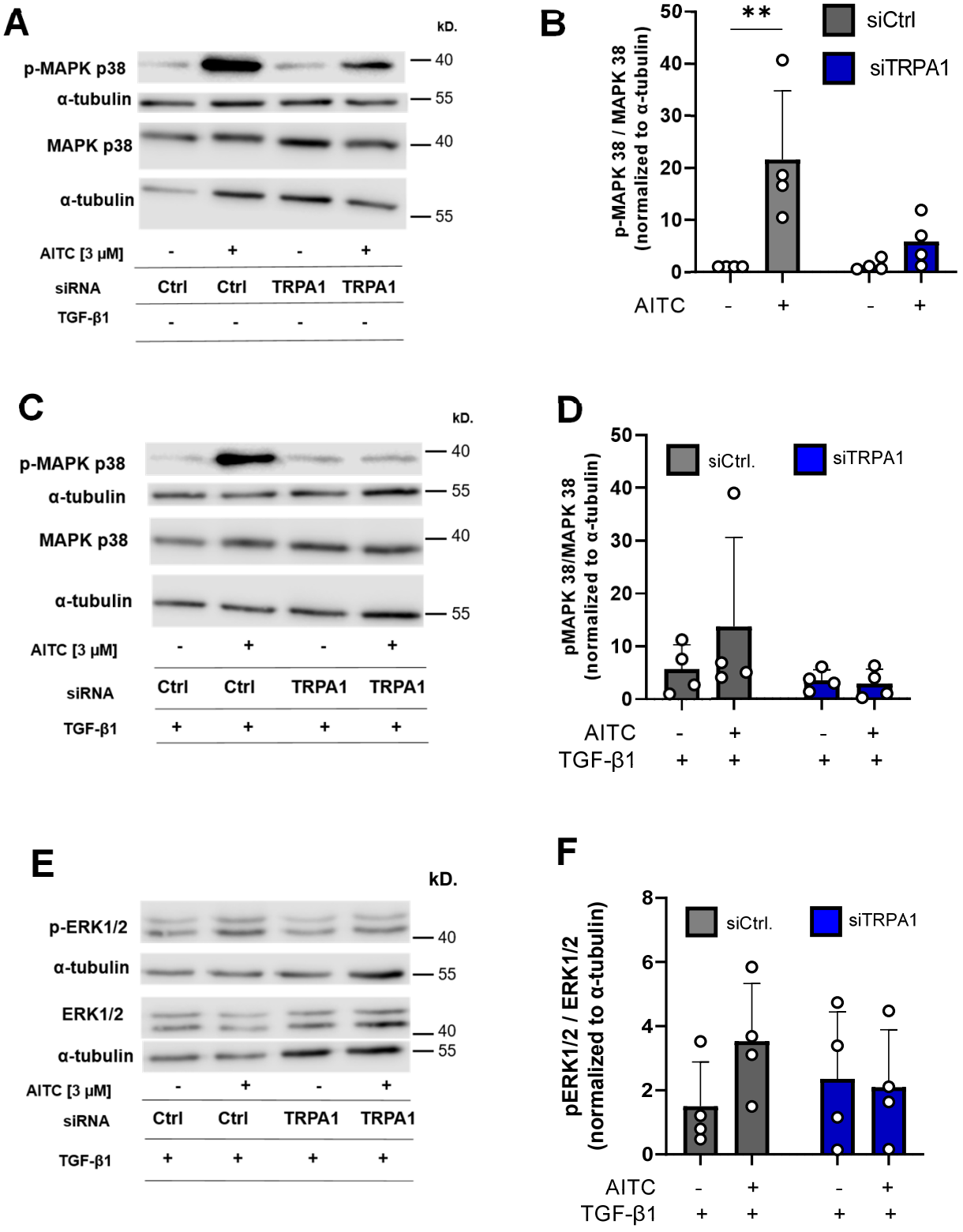
A
kD.
p-MAPK p38
α-tubulin
MAPK p38
α-tubulin
40
55
40
55
AITC [3 μM] - + - +
siRNA Ctrl Ctrl TRPA1 TRPA1
TGF-β1 - - - -
B
p-MAPK 38 / MAPK 38 (normalized to α-tubulin)
**
siCtrl
siTRPA1
50
40
30
20
10
0
AITC - + - +
C
kD.
p-MAPK p38
α-tubulin
MAPK p38
α-tubulin
40
55
40
55
AITC [3 μM] - + - +
siRNA Ctrl Ctrl TRPA1 TRPA1
TGF-β1 + + + +
D
pMAPK 38/MAPK 38 (normalized to α-tubulin)
siCtrl.
siTRPA1
50
40
30
20
10
0
AITC - + - +
TGF-β1 + + + +
E
kD.
p-ERK1/2
α-tubulin
ERK1/2
α-tubulin
40
55
40
55
AITC [3 μM] - + - +
siRNA Ctrl Ctrl TRPA1 TRPA1
TGF-β1 + + + +
F
pERK1/2 / ERK1/2 (normalized to α-tubulin)
siCtrl.
siTRPA1
8
6
4
2
0
AITC - + - +
TGF-β1 + + + +

Figure E5

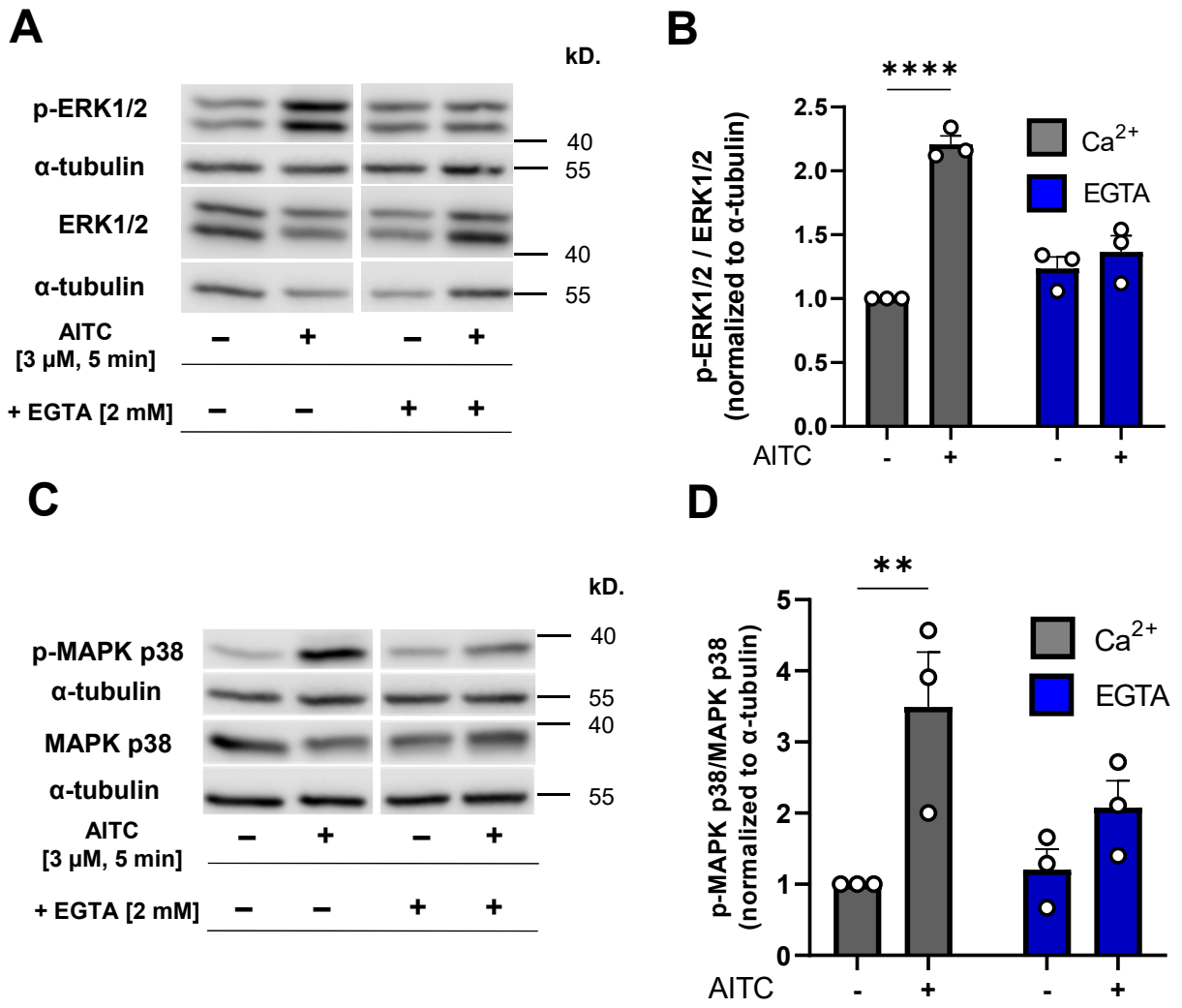
A
kD.
p-ERK1/2
α-tubulin
ERK1/2
α-tubulin
40
55
40
55
AITC
[3 μM, 5 min]
+ EGTA [2 mM]
B
****
p-ERK1/2 / ERK1/2
(normalized to α-tubulin)
2.5
2.0
1.5
1.0
0.5
0.0
Ca2+
EGTA
AITC
C
kD.
p-MAPK p38
α-tubulin
MAPK p38
α-tubulin
40
55
40
55
AITC
[3 μM, 5 min]
+ EGTA [2 mM]
D
**
p-MAPK p38/MAPK p38
(normalized to α-tubulin)
5
4
3
2
1
0
Ca2+
EGTA
AITC

Figure E6

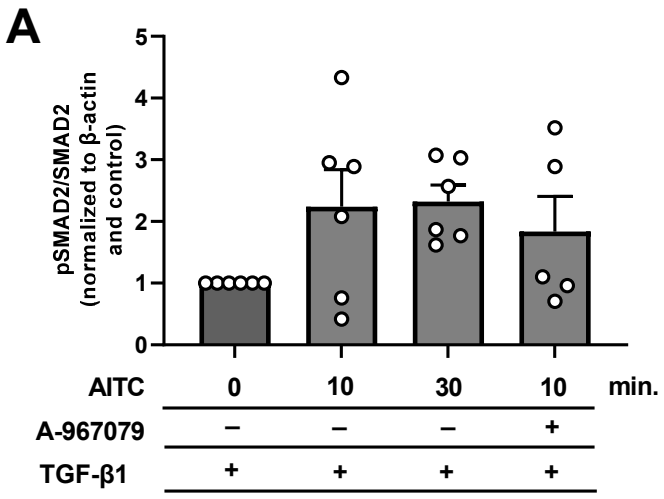
A
pSMAD2/SMAD2
(normalized to β-actin
and control)
5
4
3
2
1
0
AITC 0 10 30 10 min.
A-967079 – – – +
TGF-β1 + + + +

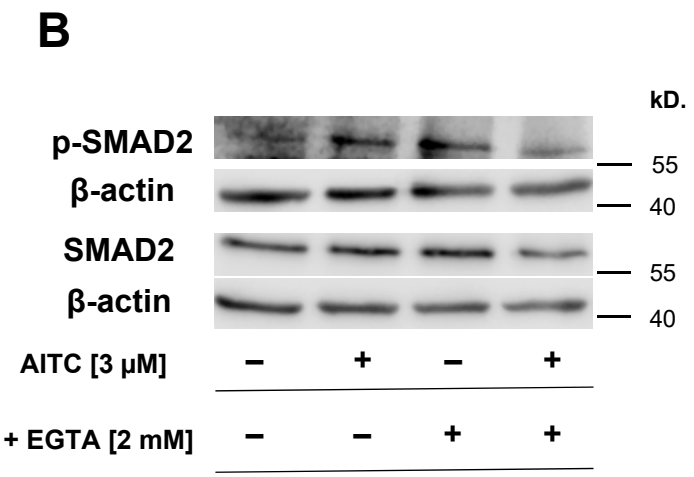
B
kD.
p-SMAD2
β-actin
SMAD2
β-actin
55
40
55
40
AITC [3 μM] – + – +
+ EGTA [2 mM] – – + +

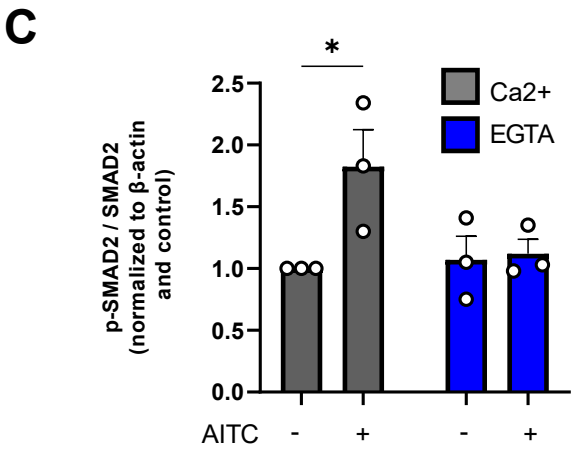
C
*
p-SMAD2 / SMAD2
(normalized to β-actin
and control)
2.5
2.0
1.5
1.0
0.5
0.0
Ca2+
EGTA
AITC - + - +

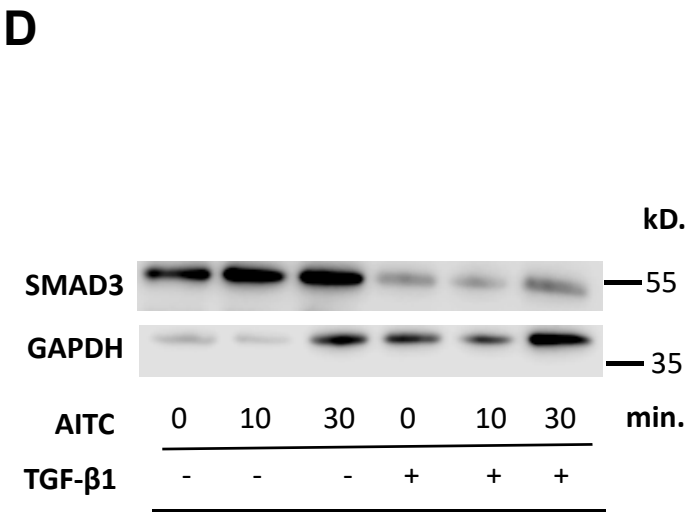
D
kD.
SMAD3
GAPDH
55
35
AITC 0 10 30 0 10 30 min.
TGF-β1 - - - + + +

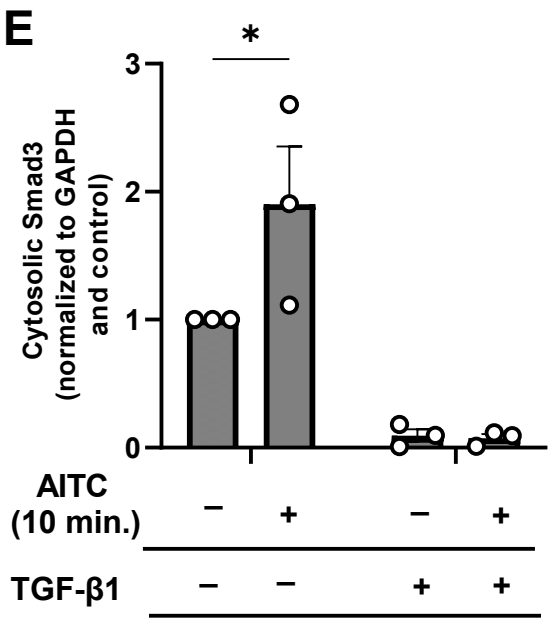
E
*
Cytosolic Smad3
(normalized to GAPDH
and control)
3
2
1
0
AITC
(10 min.) – + – +
TGF-β1 – – + +

Figure E7

A

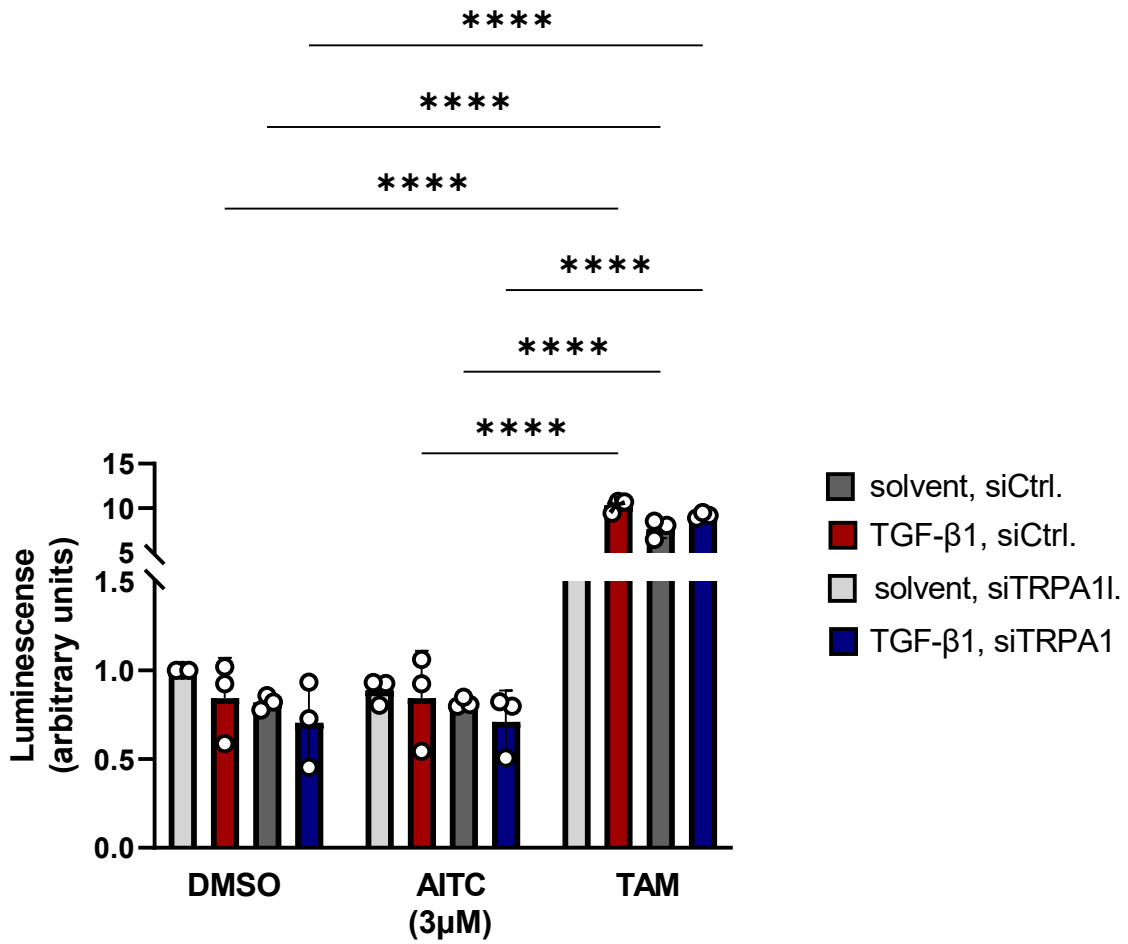
****
****
****
****
****
****
Luminescense (arbitrary units)
15
10
5
1.5
1.0
0.5
0.0
DMSO
AITC (3µM)
TAM
solvent, siCtrl.
TGF-β1, siCtrl.
solvent, siTRPA1l.
TGF-β1, siTRPA1

B

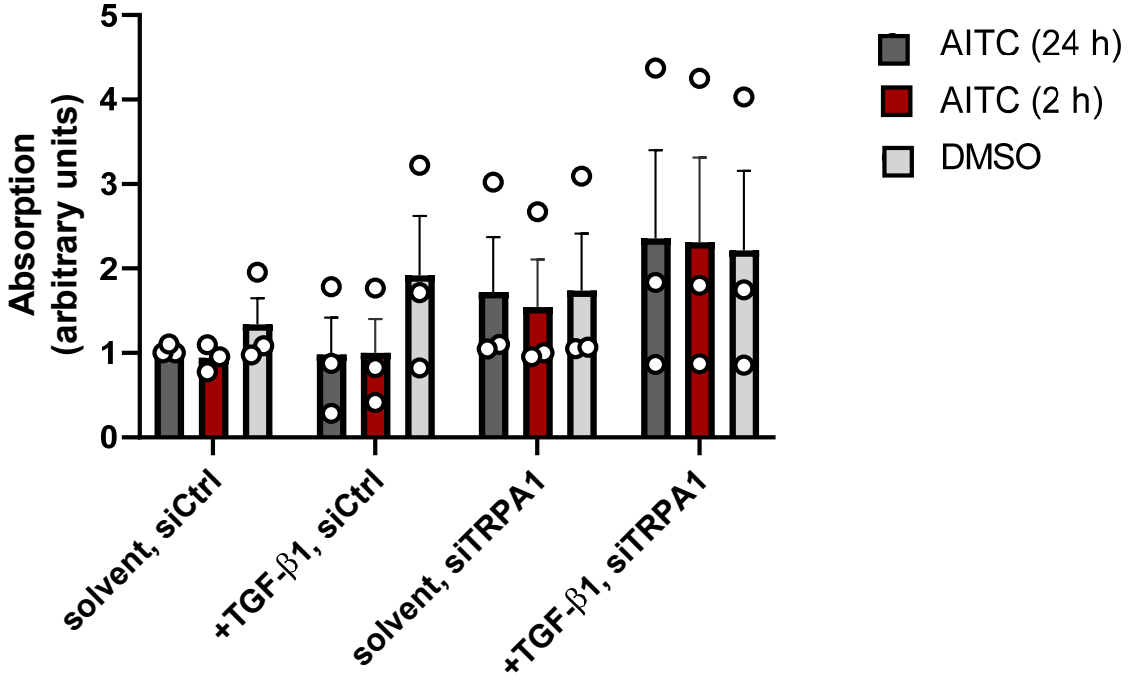
Absorption (arbitrary units)
5
4
3
2
1
0
solvent, siCtrl
+TGF-β1, siCtrl
solvent, siTRPA1
+TGF-β1, siTRPA1
AITC (24 h)
AITC (2 h)
DMSO

Figure E8